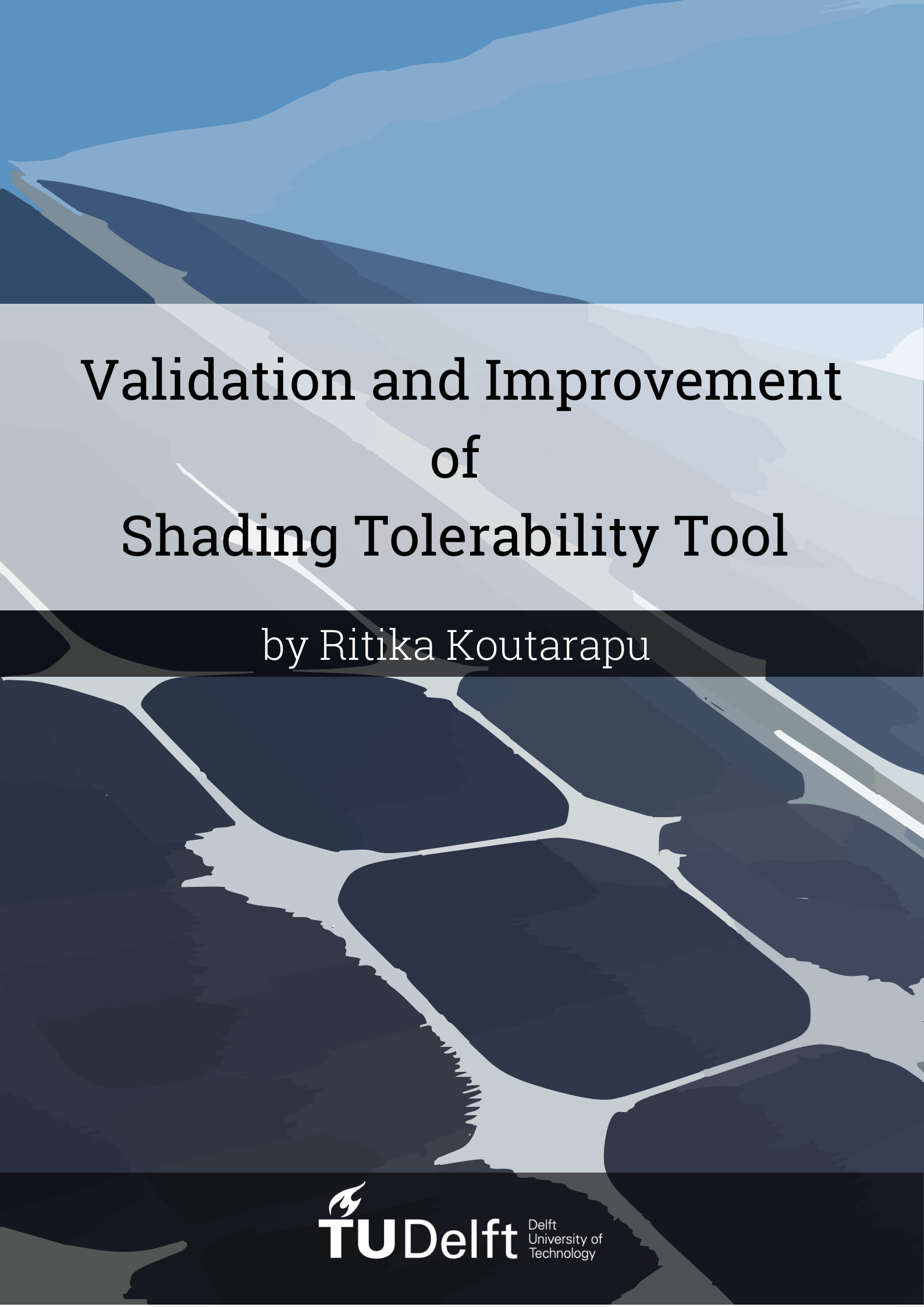

Validation and Improvement of Shading Tolerability Tool

by Ritika Koutarapu

TU Delft Delft University of Technology

Validation and Improvement of Shading Tolerability Tool

by

Ritika Koutarapu

To obtain the degree of Master of Science at the Delft University of Technology,
To be defended publicly on Wednesday, September 27, 2023 at 13:00

Thesis Committee:	Professor Arno Smets	Internal Committee Member
	Dr. Ir. Rik Versendaal	External Committee Member
	Dr. Ir Hesan Ziar	Supervisor
	Ir. Alba Alcañiz Moya	Daily Supervisor

Style: TU Delft Report Style, with modifications by Daan Zwaneveld

TU Delft

Summary

With the increase in Photovoltaics (PV) installations worldwide, PV modules are being installed more and more in urban environments which can be often subjected to high shading. Given these circumstances, the choice of a module that can withstand shading as well as possible is of paramount importance. However, there is currently no parameter to rate and compare the performance under shading of PV modules.

A probabilistic approach was developed in the literature to compute the shading tolerability (ST) of PV modules and help with this problem. Based on this concept, the basis for a tool that computes the ST of any module by using only datasheet parameters was developed. The objective of this project is to continue the development of this tool and validate it via experimental tests. Once completed, the tool will be employed to create a database for commercial PV modules and provide guidelines to achieve a high ST.

The model was first adapted from running at a sectional resolution of 12 sections to calculating ST for cell-level calculations. The results obtained for cell-level resolution are then compared to the ones obtained for 12 sections and its impact on ST is studied. To further understand the impact PV characteristics can have on ST, sensitivity analysis were carried out for breakdown voltage, nominal operating cell temperature and bypass diodes, with bypass diodes showing a positive impact on the ST value. Guidelines were made based on the sensitivity analysis to improve the performance of PV modules under shading and to improve ST of the module.

Contents

List of Figures

List of Tables

1 Introduction

Solar energy is the energy available as radiation and heat from the sun [2]. Photovoltaics is the method used to convert solar energy into other forms of energy like electricity and heat. Solar cells are photovoltaic devices that can directly convert solar energy into electricity [3]. Solar cells are placed together to form a solar module that can then be installed on rooftops, on the ground or on floating structures in lakes and oceans [3].In the last few years, a higher presence of photovoltaic (PV) systems can be observed on rooftops, on top of commercial buildings, on the ground or even on floating structures in lakes and oceans. Compared to other renewable energy sources such as wind and geothermal energy, solar energy is the easiest to integrate into urban areas [3]. This is due to their easy plug-and-use framework type and scale-able nature.

In a report by the International Energy Association, it is estimated that approximately 25 million household units use 130 GW of PV systems as of 2022 [4]. As per the Net Zero Emissions by 2050 Scenario, the number of household units employing PV systems should be more than 100 million by 2030. Correspondingly, of all PV installations done globally, 40% of them are used as 'distributed applications' in buildings and households, mainly as rooftop-based applications [4]. PV installations can be further integrated into urban areas by the addition of on-site energy storage units, easing the burden on the electricity grid and lowering the electricity bills of companies and households [3, 4].

With dropping installation costs and a set precedent of solar module use on rooftops, PV installations are being incorporated increasingly in urban areas [4]. However, the output of these PV installations is dependent on variables such as irradiation, ambient temperature and the environment the module is in. Urban areas have a high occurrence of utility structures such as scaffolding, electrical transformers, air conditioning units, satellite dishes and the like that can create shadows on PV modules, causing them to receive non-homogeneous solar irradiation, a scenario known as partial shading [5]. Partial shading conditions negatively impact the performance of PV modules.

1.1. Impact of Shading

As discussed above, some external factors can impact the performance of solar modules. One such factor is partial shading conditions [6].

When a PV module receives uniform irradiance, each solar cell generates the same current and the output power is equal to the value of the single peak in the power-voltage characteristic curve of the module, with the peak being the maximum power output the PV module is capable of [6]. This is shown by the red curve of the Power versus Voltage graph in figure 1.1 [7]. The foremost impact of shading on PV modules is loss of power. When a solar cell experiences shading, it receives less irradiance than its unshaded neighbours and will correspondingly generate less current. As solar cells are generally connected in series and hence must conduct the same current, all solar cells are forced to carry the lower current, which is the current generated by the shaded cells, and the output power is thus less than what would otherwise be achieved [5, 7]. This loss of power is shown by the shaded I-V and P-V

characteristic curves in figure 1.1 [7].

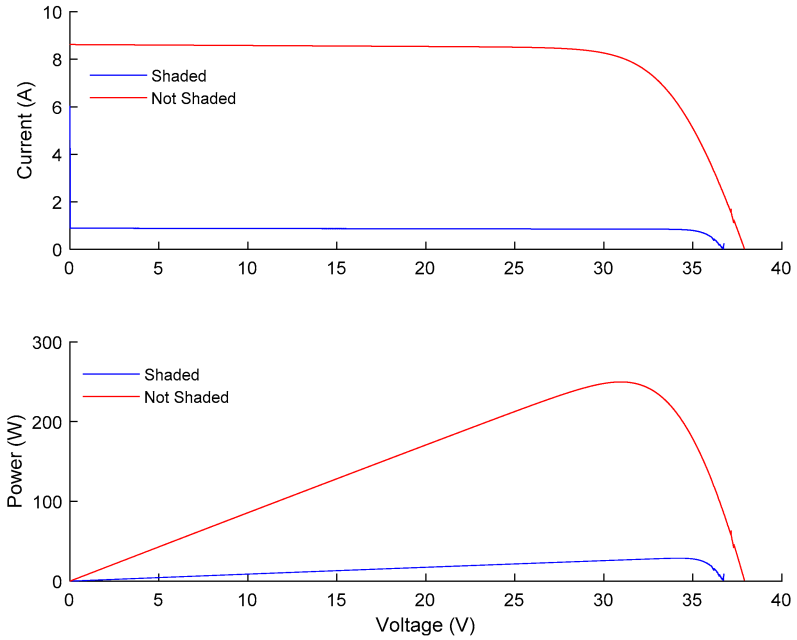

Figure 1.1: I-V and P-V curves of shaded and unshaded PV module without the use of bypass diodes [7]

This loss in power that is due to the mismatch in the output currents of the solar cells in the PV module is known as mismatch losses [2, 5].

Another impact of shading is the formation of hotspots in a PV module [6]. A hotspot is a failure condition that is characterized by part of a solar cell or a PV module having a higher temperature than its surroundings [7]. When a solar cell is shaded and limits the current in the entire series, the higher current generated by the unshaded solar cells increases the voltage in them which then reverse biases the shaded solar cells as the current from unshaded cells flows through them. The shaded cells now act as loads and the power dissipated in them raises the cell temperature and creates hotspots that can cause permanent damage [2, 6, 8].

The primary solution to these two problems is using bypass diodes that will allow an alternate path for the unshaded current. Figure 1.2 shows how a bypass diode provides a bypass for the unshaded current.

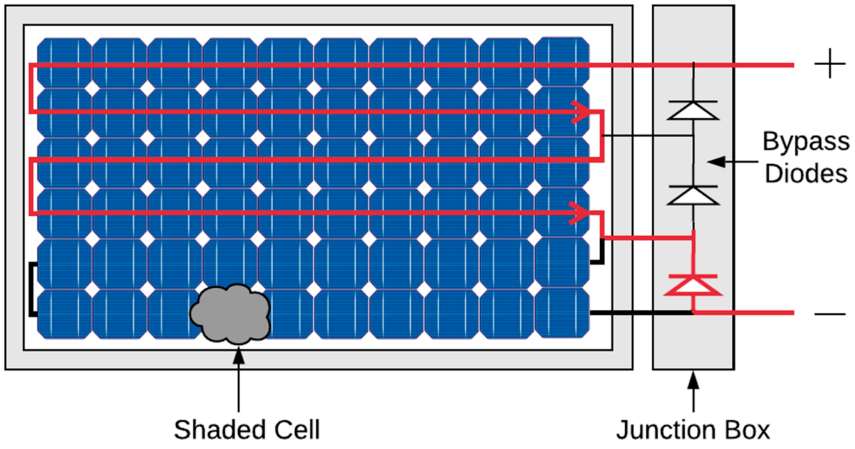

Figure 1.2: PV module with one shaded cell and one activated bypass diode [7]

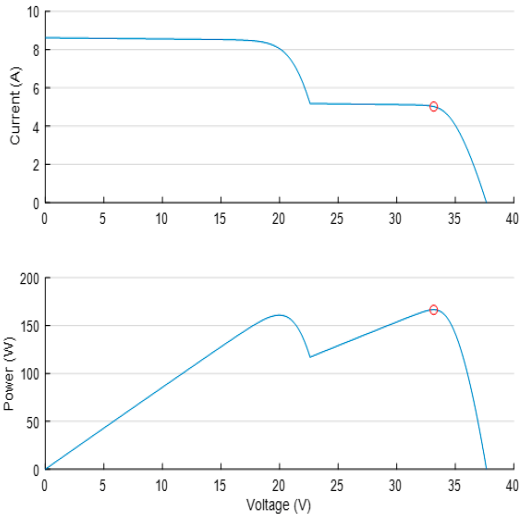

[H]

Figure 1.3: I-V and P-V curves of a shaded PV module with one bypass diode activated [7]

When a shaded cell becomes reverse-biased, it will activate the bypass diode and it will conduct the current generated by the unshaded solar cells [7]. The I-V and P-V curves of the shading scenario represented in figure 1.2 are shown in figure 1.3.

While bypass diodes do reduce the occurrence of hotspots, they are not entirely effective and further cause the formation of multiple local peaks in the power curve as seen in figure 1.3. This complicates the search for the maximum power point and can further reduce the module's performance [6, 8, 9].

The last impact of partial shading is on the rate of ageing of a solar module. All PV modules age with time and show a decrease in efficiency. However, for modules that undergo repeated exposure to partial shading, the prolonged effects of hotspots and thermal instability impact the rate of degradation and the efficiency of the module declines faster than anticipated [10, 11].

Partial shading thus has a significant impact on the performance of a PV module. Partial shading has been shown to affect up to 25% of the performance ratio (the measure of actual energy output to the theoretical energy output) of a PV module. Furthermore, depending upon the module design and orientation, partial shading substantially reduces the energy yield of the PV module [12, 13, 14]. Due to the impact of partial shading on the energy output, the ability of a module to tolerate shading is an important factor when choosing PV modules for shade-prone sites which are often found in urban environments.

1.2. Shading Tolerability (ST)

In the absence of a defined parameter, PV module data sheets use qualitative terms like "shade tolerant", "better shading response", "outstanding low light behaviour", and "excellent performance even when partially shaded" [12] to characterize the shading behaviour of PV modules. However, to form an unbiased opinion and compare modules solely based on their shading response, it becomes essential to establish a measurable parameter capable of categorizing PV modules. In 2017, Ziar et al. introduced a quantified numerical parameter, shading tolerability (ST) [12]. In this section, the calculation behind the parameter will be explained.

Due to the randomness of shading, which depends on the weather, the surroundings, and the varying power output caused by the electrical characteristics of the PV module, a probabilistic approach was chosen [12]. In probability theory, we first need to define a sample space for a random trial, which is the collection of all possible scenarios [15]. However, in the case of shading a module, we have an infinite number of possibilities with respect to shading profiles. To work more effectively, the following

two assumptions are made by Ziar et al.

1. Irradiation across the surface of a PV cell is homogeneous and can have a value between 0 and 1 kW/m^2
2. The chances of shading PV cells are equal and independent of their location in the PV module (or the location of the module in an array)

Working under the above assumptions, for i possible irradiation levels and c cells, total number of shading scenarios will be i^c. As there are infinite irradiation levels between 0 and 1 kW/m^2, each unique shading pattern has a $\lim_{i\to\infty} 1/i^c$ possibility of occurring. With this, we have now established our sample space [12].

The shading tolerability parameter (ST) is defined as the "mathematical expectation of power production". The mathematical expectation is the product of the probability of an event occurring and the value corresponding with the actual observed occurrence of the event. Thus a higher mathematical expectation of ST indicates a higher shade tolerance and the value can be used to compare PV modules [12, 15].
For a random variable x with a possibility of occurring $p(x)$, expected value is:

$$E(x) = \sum_{k=1}^{\infty} x_k \cdot p\left(x_k\right) \tag{1.1}$$

Using equation 1.1, ST of a PV module can be calculated as

$$ST_{(i,c)} = \frac{1}{P_{mod,mpp}} \sum_{k=1}^{k=i^c} P_k \left(\frac{1}{i^c}\right) \tag{1.2}$$

where $ST_{(i,c)}$ stands for shading tolerability, $P_{mod,mpp}$ is the nominal power point of the module, and P_k is the power at the MPP of the module for every shading scenario. $P_{mod,mpp}$ is used to normalize the value to allow the comparison of PV modules with different rated power.

1.3. Thesis Objectives

Past research done on shading tolerability focused on evaluating the parameter for specific PV modules experimentally [12, 16] or by running simulations for specific PV modules under selected shading scenarios [17]. Due to the time constraint of an experimental set-up, evaluation is possible only at a low resolution (i = 2 irradiation levels and c = 6 sections) and for a few PV modules. Furthermore, a lab set-up requires access to the PV modules itself which makes it impossible to set up a database.

Work done by Nida et al. focused on overcoming these challenges by creating a MATLAB-based tool that could calculate the ST parameter relatively quickly [1]. The created MATLAB tool would calculate the ST for any PV module at double the resolution of the work done by Ziar et al. and Mishra et al. (c = 12 sections). This work aims to build upon the progress already made by Nida et al.

The focus of this thesis is to

- Optimize the MATLAB-based ST calculator
- Improve the resolution of the MATLAB tool to calculate ST for higher c values and study the impact of it on the ST parameter
- Study the relation of certain PV module parameters on the ST parameter by isolating their impact
- Find guidelines to improve the shade tolerance of PV modules

1.4. Thesis Outline

In this report the following layout is followed,

- Chapter 2 gives an overview of basic PV concepts that are required to understand the work done in the report and the literature review.

- In Chapter 3 it is explained how the development and adaptation of the MATLAB-based ST calculator was done and the differences that are seen in the shading tolerability values after these changes.
- In Chapter 4 The validation process, the experimental results and its analysis are covered.
- Chapter 5 covers the sensitivity analysis done in the MATLAB-based calculator and the results obtained from it
- Chapter 6 reports the final conclusion and recommendations made by this report.

2

Literature Review

This chapter will discuss concepts about the workings of a PV module, the conceptualisation of the shading tolerability parameter and its calculation in the literature. Section 2.1 covers the working of the PV module, followed by section 2.2, which will discuss the prior work done on the shading tolerability parameter, including the experimental measurement of ST and modelling of ST. The final section 2.3 covers the work done to develop a MATLAB-based ST calculator.

2.1. PV Concepts

To understand how shading conditions impact module performance, it is required to comprehend how the module performs in terms of power and how the module's layout contributes to this.

2.1.1. Maximum Power Point and the I-V curve

The maximum power a module can deliver under Standard Test Conditions (STC) of 1,000 W/m^2 solar irradiance, 25° C cell temperature, air mass(AM) equal to 1.5, is the rated maximum power given on the datasheet of a module [18]. Different shading profiles generate different I-V curves and often have peaks occurring due to the presence of bypass diodes as discussed in 1.1 and shown in the figures 1.1 and 1.3. Keeping track of this MPP allows maximum power to be delivered to the load and improves the efficiency of the PV module under shading conditions [19, 18].

A PV cell's current and voltage characteristics are shown by plotting an I-V curve. The current that flows through the external circuit when the electrodes in a PV module are short-circuited is defined as the short-circuit current I_{sc}. On the I-V curve, I_{sc} is the point where the curve intersects the y-axis. The

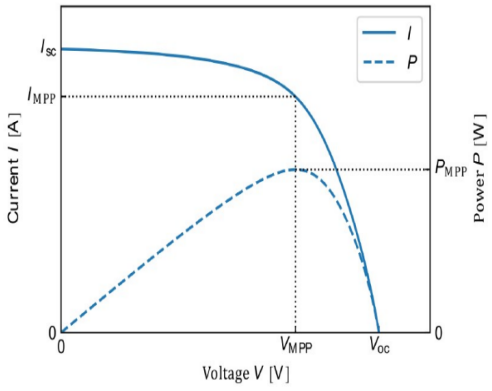

Figure 2.1: I-V curve of an ideal solar cell

I_{sc} generated depends on the irradiance falling on the solar cell. Thus, I_{sc} is directly dependent on the area of a solar cell [19].

The voltage at which no current flows through the external circuit is defined as the open-source voltage V_{oc}. On the I-V curve, V_{oc} is the point where the curve intersects the x-axis. The point at which power generated from the PV module is maximum is defined as the maximum power point (MPP). The power at this point is also called the nominal power or the operating power of a PV module, identified as P_{mpp}. This is the power provided by the PV module under standard test conditions and is affected by external factors such as temperature and irradiance, as current and voltage are also affected by these factors [19]. As shown in figure 2.2, when the irradiance decreases, the current decreases and the voltage is slightly affected, while when the temperature is increased, the voltage drops, and the current slightly increases.

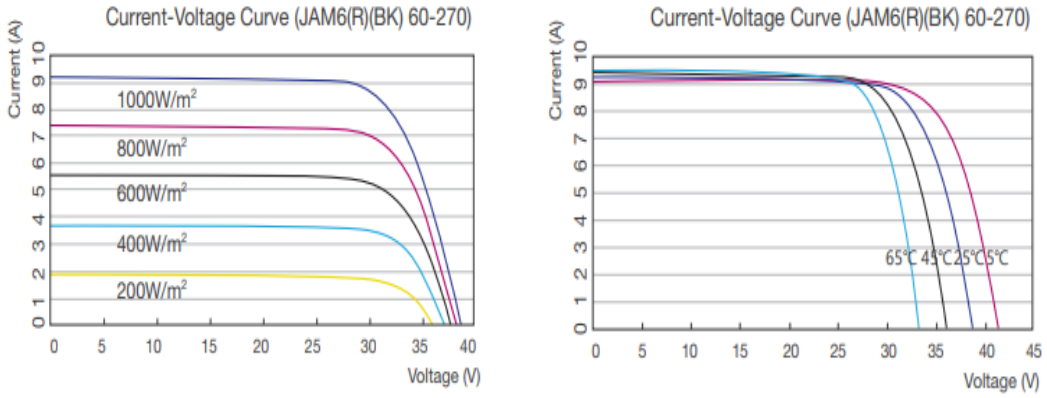

(a) I-V curve: Impact of irradiance [20].

(b) I-V curve: Impact of temperature [20].

Figure 2.2: I-V curve of JASolar 60 cell, 275W module.

2.1.2. Series and Parallel interconnections and bypass diodes

Solar cell interconnections can be in series or parallel. An example of the I-V curve for both series and parallel connections is shown in figure 2.3.

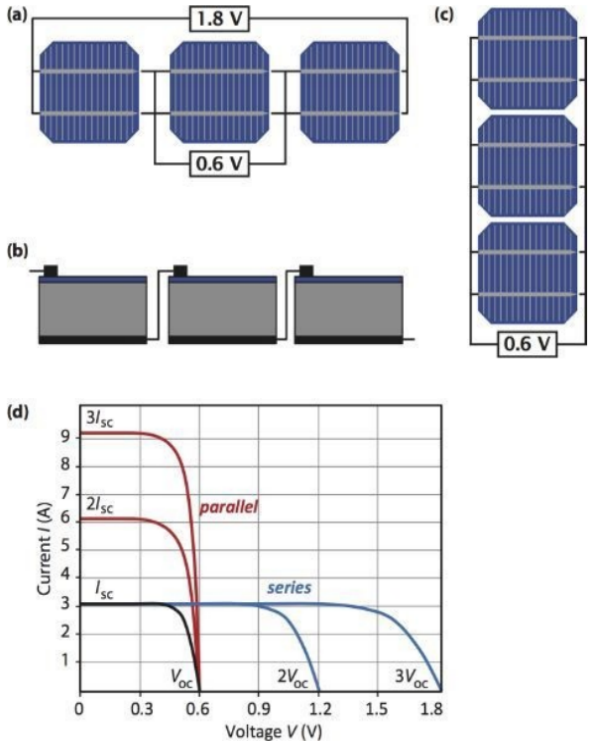

Figure 2.3: : (a) A series connection of three solar cells; (b) realisation of such a series connection for cells with a classical front metal grid. (c) A parallel connection of three solar cells. (d) I-V curves of solar cells connected in series and parallel [19]

In the case of cells connected in series, the individual currents do not simply sum up together, but the voltage of the cells sums up. Instead, the overall current in the entire series is dictated by the cell producing the least current. Consequently, the total current in a string of solar cells equals the minimum current produced by a single solar cell. This can be problematic when even a single cell in a string is shaded, limiting the current to that generated by the shaded cell [19].

If solar cells are connected in parallel, the voltage remains the same, but the current adds up. However, we cannot connect all cells in parallel as the increased current will cause a significant loss of power due to series resistance. A simple way of using a series and parallel connection in a PV module is shown in figure 2.4.

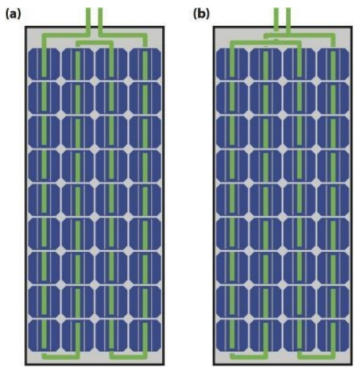

Figure 2.4: A PV module consisting of (a) a string of 36 solar cells connected in series; and (b) two strings each of 18 solar cells connected in parallel [19].

Conventionally, solar cells are connected in series with 3 bypass diodes connected in parallel to reduce the impact of shading by providing an alternative path to the current to pass through. This is described

in chapter 1. The half-cell layout is an example of utilising series and parallel interconnection with a bypass diode is the half-cell layout. In the figure 2.5.

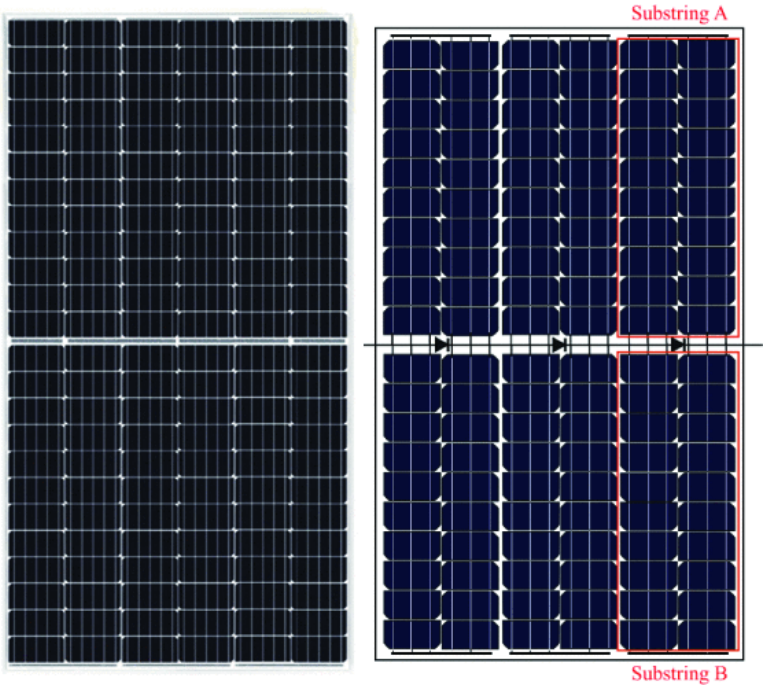

Figure 2.5: Half-cell PV module with six substrings and three bypass diodes

2.2. Literature Review

This section covers the previous work done on the shading tolerability parameter and how the module performance is impacted by shading and looks into the possible relation of shading and PV module parameters.

2.2.1. Ziar et al.

Ziar et al. introduced ST as a parameter that can be measured and conducted experimental calculations for several modules. This section 1.2 takes a look at how they arrive at equation 1.2, which calculates ST for a PV module. Ziar et al. found the general equation of ST to be:

$$\mathrm{ST}_{(i,c)} = \left(\frac{m}{c}\right)\left(\frac{1}{i^n}\right)\left[\sum_{k=1}^{k=j}\left(\frac{n}{j}\right)k + \sum_{a=1}^{a=j-1} n\left(\frac{j-a}{j}\right)\sum_{b=1}^{b=n-1}\binom{n}{b}a^{n-b}\right] \tag{2.1}$$

where n is the number of cells in series, m is the number of strings in the PV module, $c = n \times m$ and $j = i - 1$. For $ST_{(i=2,c)}$, the equation simplifies to:

$$\mathrm{ST}_{(i=2,c)} = \left(\frac{1}{2^n}\right) \tag{2.2}$$

For two PV modules, Module 1 and Module 2, given that $ST_{(i=2,c)}$ is greater for Module 1 than Module 2, then $n_1 < n_2$ based on equation 2.2. As $n_1 < n_2$, then from equation 2.1 we get that $ST_{(i\to\infty,c)}$ is also greater for Module 1 compared to Module 2. Naturally, as

$$\mathrm{ST}^{(\text{module }_1)}_{(i=2,c)} > \mathrm{ST}^{(\text{module }_2)}_{(i=2,c)} \Rightarrow \mathrm{ST}^{(\text{module }_1)}_{(i\to\infty,c)} > \mathrm{ST}^{(\text{module }_2)}_{(i\to\infty,c)} \tag{2.3}$$

it proves that using $ST_{(i=2,c)}$ is valid in place of $ST_{(i\to\infty,c)}$.

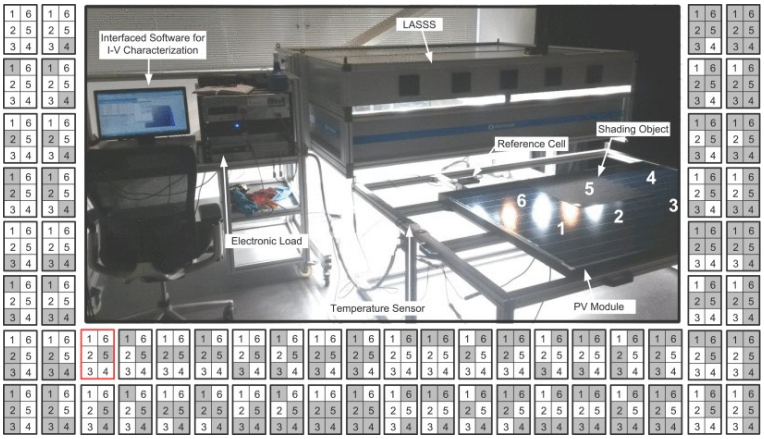

Figure 2.6: Indoor experimental setup for testing shading tolerability along with 64 shading profile codes from 000000 to 111111

Experimentally, equation 1.2 cannot be calculated due to levels of irradiance approaching infinity between 0 to 1000 W/m^2. By utilizing equation 2.3, Ziar et al. were able to measure $ST_{(i=2,c)}$ experimentally. With the number of potential scenarios equating to 2^c, this quantity increases exponentially with higher values of c. As the count of potential scenarios grows, the corresponding number of necessary tests and the subsequent measurement time also increases, posing a disadvantage to the industrial application of ST [12]. Instead, modules were split into six geometrically equal sections, as it is easy to divide the surface of a PV module into 3×2 sections while accounting for how the solar cells are connected, in series or parallel. For $c = 6$, the number of possible scenarios is $2^6 = 64$, which is a far more manageable number. The 64 possible scenarios can be seen in the figure 2.6

Experimental ST calculations were carried out for 11 PV modules, with the PV modules selected to cover a range of technologies, number of cells, and bypass technologies. On average, it took 5.73h to carry out each measurement, and in total, it took 63.11h to measure all 11 modules [12]. The two irradiance levels selected were 1000 W/m^2 for the unshaded region and 250 W/m^2 for the shaded region. A shaded irradiance of 250 W/m^2 was chosen to replicate shadows caused by diffuse irradiation in natural conditions. The EternalSun large area steady state solar AAA-class (AM 1.5) simulator was used to simulate the applied irradiance and measure the I-V characteristics for every scenario [12].
The experimental work carried out in the indoor testing for the 11 chosen PV modules showed that the two modules with the highest ST value outperformed two other modules with one bypass diode per cell. It was concluded that the number of bypass diodes alone cannot be considered a sole criterion for comparing ST. It should be noted that these experiments were carried out at c=6 sectional resolution and may not carry over if done at cell-level resolution.

2.2.2. Mishra et al.

In the work done by Mishra et al., ST was again measured experimentally for four PV modules with the same experimental setup of $c = 6$ sections and shaded and unshaded irradiance levels of 250W/m^2 and 1000W/m^2, respectively. ST was measured experimentally at three different ambient temperatures of 25° C, 30° C, and 35° C with the aim to find if ST is an innate property of a PV module by searching for any correlation between ST and ambient temperature [16].

Using the NOCT model, the effect of temperature was analytically calculated in combination with the temperature coefficient for power γ. On average, change in %ST was found to be 0.07 %ST/° C. ST is concluded to be almost independent of ambient temperature due to the negligible difference in the value of ST.

2.2.3. Klassen et al.

The work done by Klassen et al. compared the impact of partial shading on four different topologies of PV modules: conventional, butterfly, shingle string, and shingle matrix. Conventional modules generally have solar cells connected in series. In contrast, a 'butterfly' layout has two additional parallel

connections, and the solar cells used are half-cut solar cells to improve shading resistance. Shingle cells take this a step further by cutting solar cells into strips and overlapping them inside the framed module. When the shingled cells are arranged in an offset manner with the solar cell connections made in a 'total-cross-tied' configuration, it has series and parallel interconnection [17].

Circuit simulations were done using the open-source code SPICE to obtain I-V characteristics of the modules under different shading scenarios [17]. For the simulations, 30 solar cells are used and are connected in a way that can represent the four different topologies selected. To compare the shading tolerability of modules, an approach similar to ST is utilised to calculate the parameter "the average normalised power for partial shading" $\bar{P}_{ps}$ [17].

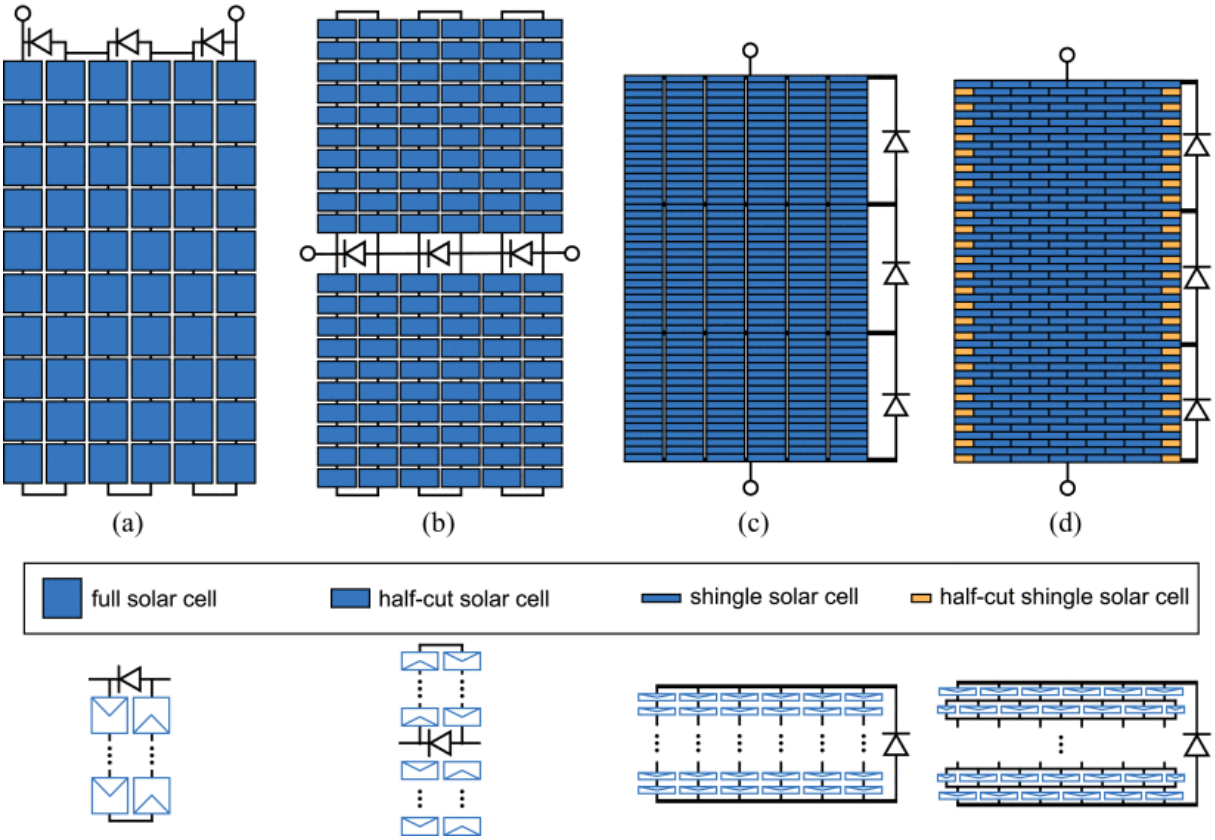

Figure 2.7: Module layouts investigated in this article, a) conventional full-sized solar cell interconnection, b) half-cut solar cell butterfly layout with centred diodes and two parallel blocks of solar cells, c) shingle string interconnection with six parallel strings of shingle solar cells intermitted by three diodes, d) shingle matrix interconnection with serial and parallel interconnection of each individual solar cell

The shading scenarios for these simulations were created using a sampling method to allow for an even distribution over the sample space. The shading shapes fall under two sets: rectangular and random. Rectangular (clustered) shading patterns categorise the shading patterns that can be caused by other solar panels and building features, such as chimneys and poles. Random (scattered) shading patterns categorise patterns with more minor obstructions, such as leaves and bird droppings. Together, they cover a significant fraction of shading scenarios that occur in urban environments.

The results for rectangular and random shading are shown in figures 2.8 and 2.9. The black arrows in the figures indicate several horizontal lines corresponding to cases where at least one bypass diode is conductive, which are visible in both graphs. However, we find a smoother slope in the results for the random sample set. It is further noted that the results were done for varying sample sizes, with the sample size increasing from 0 to 1200 for rectangular and random each. The average normalised power values showed approximately the same values once the sample size increased above 200 scenarios, concluding that 200 scenarios could be deemed sufficient.

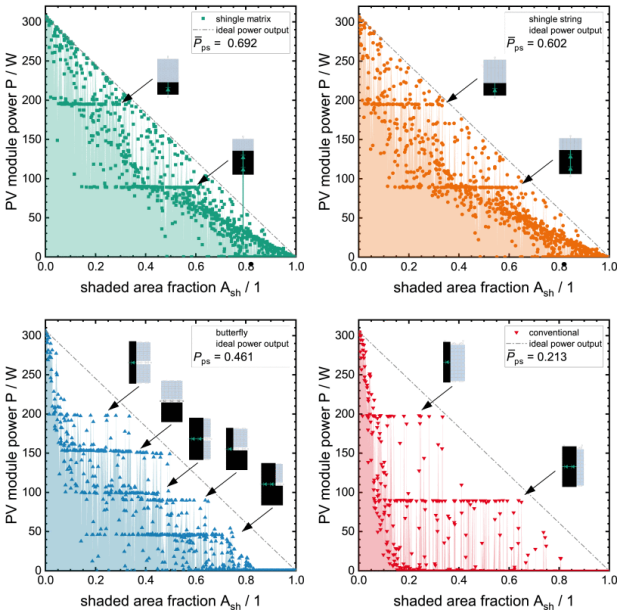

Figure 2.8: Results of the study done for rectangular shadows. Each graph contains the data points for one module layout with its ideal power output as a dash-dotted line. The area below P(Ash) is highlighted and $\bar{P}_{ps}$ computed.

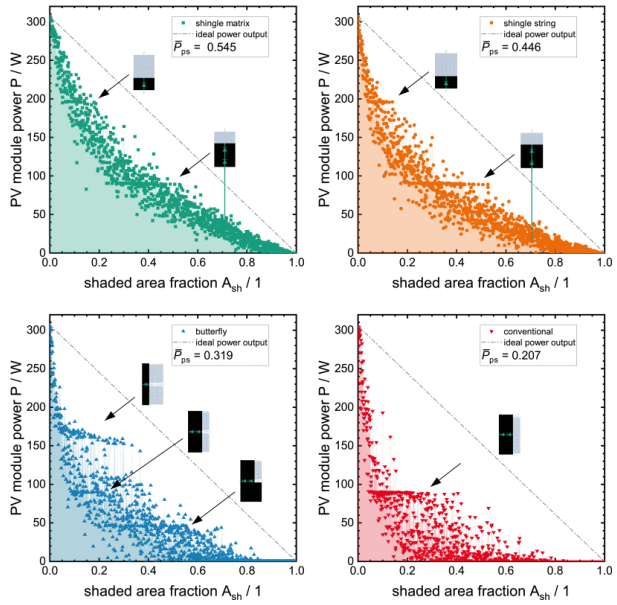

Figure 2.9: Results of the study done for random shading of PV modules. Each graph contains the data points for one module layout with its ideal power output as a dash-dotted line. The area below P(Ash) is highlighted and $\bar{P}_{ps}$ computed. We find less distinct horizontal lines compared to rectangular shading corresponding to bypass diode in conductive states.

2.2.4. Nida et al.

The research shown above evaluated ST experimentally or by running simulations on representative models. Experimental work was additionally limited by time constraints, the limit in the number of sections, and the obtaining of the PV modules [12, 16]. The work done by Nida et al. focused on creating a MATLAB-based ST calculator that was relatively quicker in calculating ST, would work for any PV module based on the data available on its datasheet, and created a database for easy comparison [1].

The work done by Nida et al. calculates ST for a PV module based on equation 1.2. While the work done by Ziar et al. and Mishra et al. previously had $2^6 = 64$ total possible scenarios when considering

two irradiance levels [12, 16]. For this work, the number of scenarios was increased as the number of geometrically equal sections was taken as $c = 12$. Therefore, there were $2^{12} = 4096$ total possible scenarios to be considered. To optimise the computational time of the model, equivalent scenarios were identified based on the module's interconnections and layout. This concept of equivalent scenarios is further explained in 2.3. The reduced number of scenarios ranged from 35 to 100, which was a significant decrease, and the simulation time was below 2 hours on average. The reduced simulation time also allowed for creating an ST database of 40 different PV modules based on the ST calculator [1].

A few drawbacks of the MATLAB model are the computational time which limited the number of sections that could be achieved. A faster computational time per module would allow one to create more sections and calculate the value of ST for a larger number of total scenarios. If the number of sections can be made to be the same as the number of cells in the PV module, the impact of module parameters can be studied. One of the research aims of this thesis is to optimise the speed of the code and adapt it to perform at cell-level resolution. To do so, we first need to understand the MATLAB tool, which is discussed in section 2.3.

2.3. MATLAB-based ST calculator

The MATLAB-based ST calculator calculates ST based on equation 1.2. This requires the tool to find all the possible shading scenarios in order to evaluate the power output of the PV module for each scenario. In the sections below, we will first briefly explain how the 12 geometric sections are divided upon a module of varying numbers of cells. This will help reduce the number of shading scenarios, as illustrated in section 2.3.2. The power output of each of these scenarios is then obtained by generating the I-V curve, which is explained in section 2.3.3. The final ST calculation is then briefly described in section 2.3.4.

2.3.1. Section details

As previously mentioned in 2.2.4, the work done by Nida et al. calculates ST for $c = 12$ sections. This is done by splitting the PV module into a 3×4 or 4×3 configuration. On dividing the module into 12 geometrically equal sections, one of the three outcomes can be obtained and can be identified in 2.10, with blue lines representing the geometrical sections and the yellow lines representing the strings distributed across 3 or 4 bypass diodes.

- **Case 1**- The sections are split completely equally with no cells cut in half (0.5 granularity) and each section lying completely within the same bypass string. This case is shown in figure 2.10 (c), and the blue and yellow lines lie on each other.
- **Case 2**- Each section still lies within the same bypass string, but each section can contain full cells and half-cut cells of 0.5 granularity. This case is shown 2.10 (b). The blue and yellow lines still lie on top of each other, but the horizontal blue lines cut some solar cells in half.
- **Case 3**- Sections can contain half-cut cells of 0.5 granularity and full cells and are also distributed across two bypass strings. This case is shown 2.10 (a), and the blue and yellow lines do not lie on each other.

From cases 1 to 3, the configurations get less symmetrical. As more symmetrical configurations are bound to have more scenarios with identical power outputs, a configuration that gives a more symmetrical outcome will reduce the count of unique scenarios and can reduce computational time. Thus, a configuration is selected when either option fits the scenarios' conditions in the following order of preference: Scenario 1 $>$ Scenario 2 $>$ Scenario 3.

2.3.2. Shading Scenarios

The total possible number of scenarios was found to be i^c by Ziar et al., where i is the level of irradiance considered, and c is the number of geometrically equal sections [12]. As discussed in section 2.2.4, for $i = 2$ and $c = 12$, we have $2^{12} = 4096$ total possible scenarios. As calculating the I-V curve and extracting the P_mpp values for these many scenarios would take 120 hrs on average per module, it is necessary to find a way to reduce this value[1].

Due to the nature of how bypass diodes work and how the configurations are chosen, as seen in section

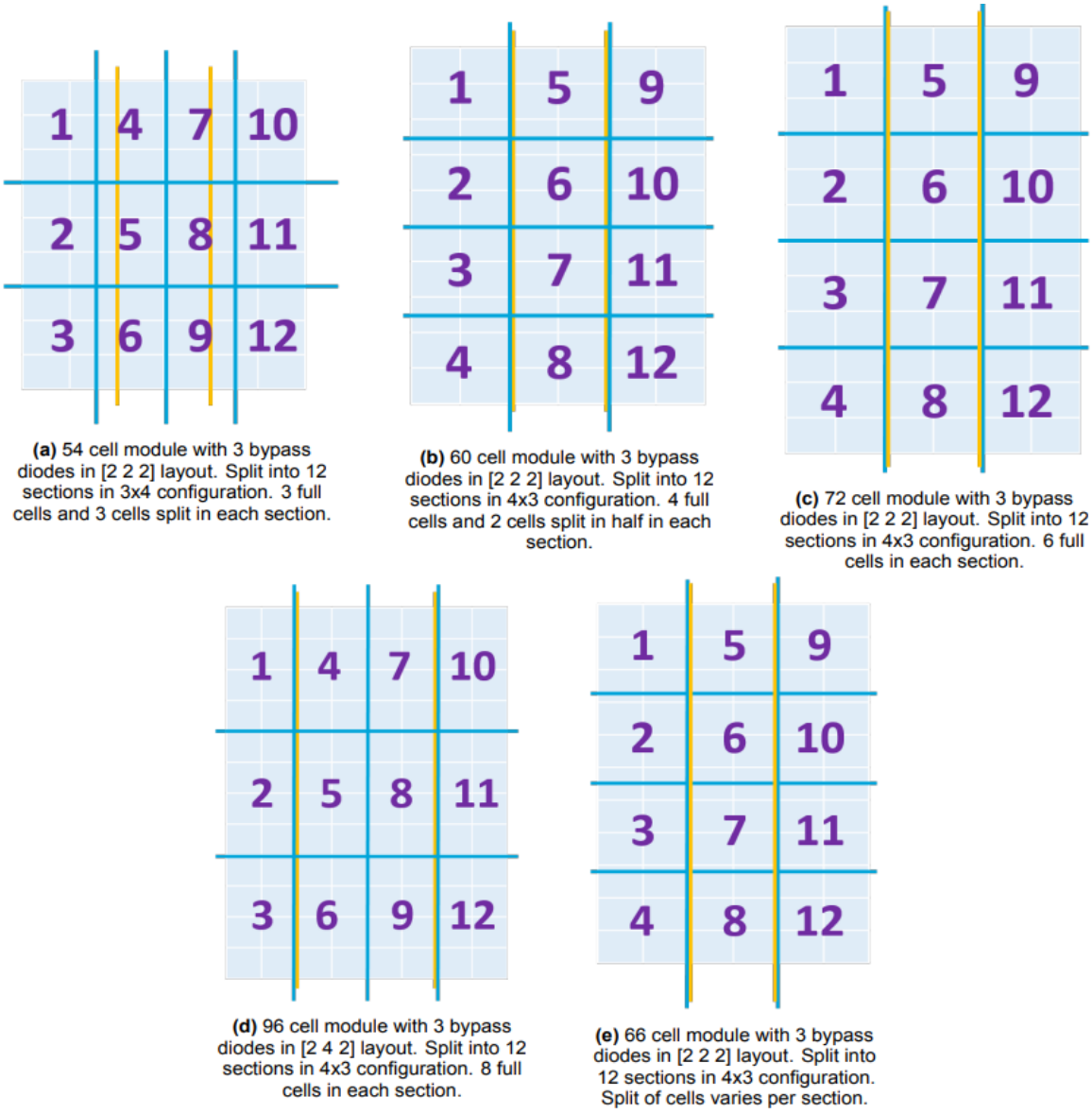

(a) 54 cell module with 3 bypass diodes in [2 2 2] layout. Split into 12 sections in 3x4 configuration. 3 full cells and 3 cells split in each section.

(b) 60 cell module with 3 bypass diodes in [2 2 2] layout. Split into 12 sections in 4x3 configuration. 4 full cells and 2 cells split in half in each section.

(c) 72 cell module with 3 bypass diodes in [2 2 2] layout. Split into 12 sections in 4x3 configuration. 6 full cells in each section.

(d) 96 cell module with 3 bypass diodes in [2 4 2] layout. Split into 12 sections in 4x3 configuration. 8 full cells in each section.

(e) 66 cell module with 3 bypass diodes in [2 2 2] layout. Split into 12 sections in 4x3 configuration. Split of cells varies per section.

Figure 2.10: Examples of splitting of various configurations of modules and resulting sections [1].

2.3.2, the arising symmetrical outcomes allow ”equivalent” scenarios to get identified and counted as one unique scenario.

2.3.3. I-V curve generator

Once the shading scenarios are identified, the P_mpp needs to be computed. To generate the I-V curve, the tool requires data that is available on a PV module's datasheet such as V_{oc}, I_{sc}, V_{mpp}, I_{mpp}, P_{mpp}, V_br, the number of bypass diodes and the temperature coefficient. The input data is adjusted to cell-level values. The two-diode model is followed to calculate the remaining parameters required. Parallel (shunt) resistance R_p and series resistance R_s are then calculated by following a simple iterative process. The two-diode module generates these parameters at the cell level. The parameters are first calculated under Standard Test Conditions (STC) of 1000 W/m^2 irradiance, AM 1.5 spectrum at 25° C. For non-STC conditions, irradiance and temperature dependency were added to the parameters. The Nominal Operating Cell Temperature (NOCT) model is used to obtain cell temperature from the ambient temperature given in the datasheet.

To get the current and voltage characteristics at the module level, a model of the series connection

of cells is made. The I-V curve is generated first for all the homogeneous conditions where all cells of the module are under the same conditions. As current and voltage characteristics are identical for every cell and all the cells are in a series condition, the current characteristics are kept the same and voltage characteristics are found by multiplying voltage with the number of cells.

Partial shading falls under non-homogeneous conditions, and the I-V characteristics of the cells are no longer identical. The current in a string is limited by the cell that produces the least current. This value of the current is then assigned to all the PV cells in series, and the corresponding voltage is calculated. The voltage characteristic of the module is found by adding up the voltage assigned to each cell in that series.

The work done by Nida et al. also includes the effects of the reverse bias voltage and the impact of bypass diodes on the I-V curve. The reverse bias region is relevant when cells become reverse biased due to the series connection requirements and partial shading. Shaded cells may operate in this region, resulting in power dissipation and potential heating. As the reverse voltage becomes more negative, the solar cell goes into reverse breakdown, and the high current achieved can lead to cell degradation and damage. Bypass diodes limit this effect of partial shading. Bypass diodes are connected in parallel across a string of series-connected solar cells. Under normal operating conditions, they exist in reverse bias and act as an open circuit. They activate when the overall voltage of the string drops below the diode's forward voltage. The reverse bias voltage of the shaded cell is now equal to the forward bias voltages of the other solar cells in the series. The I-V curves can be modelled for the module and be used to calculate further the P_{mpp} values for every scenario.

2.3.4. ST calculator

Once all the ingredients are ready, we can compute the ST. The scenario matrix is found first and contains all the final unique scenarios and the number of times each scenario occurs. For calculating ST, irradiance matrices are created for all scenarios using the scenario matrices that were found previously, with each section having an irradiance of 1000W/m^2 or 100W/m^2. The cell-temperature matrix is calculated using the irradiance matrix to identify shaded and unshaded cells for every scenario. The temperature of every cell is then calculated using the NOCT model, as mentioned above. The I-V characteristics are calculated next using the irradiance matrices, the temperature matrices and the I-V characteristics generated at cell-level. ST can be calculated with the final output of P_{mpp} values of the unique shading scenarios and the number of times each unique scenario repeats.

3

ST Code for Cell-Level

Section 2.3 explains the process by which the required parameters (P_{mpp} values of each scenario, number of unique scenarios, and number of times each scenario repeats) are obtained to calculate the ST value for when a module is divided into 12 sections. In this chapter, we focus on the thesis objective of adapting the MATLAB-based ST code to work for section cell-level resolution. The first section 3.1 explains the modifications performed for this purpose. Section 3.2 compares both ST strategies for commercial PV modules.

3.1. Adapting ST calculator to Cell-level Resolution

The total number of possible shading scenarios for two irradiance levels ($i = 2$) is given by the equation 2^c. At cell-level resolution, the number of sections can be of any value, like c=48 and c=96, or even c=144, depending on the number of cells the selected PV module contains. The total number of scenarios will increase drastically with the value of c increased. For example, at c=60, the value of 2^{60} is in the order of 10^{18}. On identifying duplicate scenarios, the number of unique scenarios at the cell level will still be in the hundreds or thousands. However, at c=12, the reduced number of unique scenarios for PV modules ranges from 35 to 100. As the code takes, on average two hours per module at c=12 resolution, it is vital to optimise the code's computational speed to work at cell-level resolution.

3.1.1. Speed optimization

It was found that the use of 'for' loops was taking considerable time as they call elements individually. If a matrix contained an extensive data set, it would prove to be time-consuming, increasing computational time. MATLAB is optimized for operations involving matrices and vectors [21]. Vectorization in MATLAB refers to the practice of performing operations on entire arrays (vectors, matrices, etc.) as a whole rather than using explicit loops to process individual elements. It takes advantage of MATLAB's optimized internal operations, leading to faster and more efficient code execution. Computational time is reduced to seconds for the calculation of ST with this change for c=12.

3.1.2. Unique Shading Scenarios

Shading scenarios are represented in the MATLAB code as a matrix, with the number of rows depending on the number of scenarios and the number of columns being the number of bypass diodes the PV module has. Thus, each element represents the number of shaded cells per bypass string.

As explained above, the number of scenarios is rather large at cell-level sectioning. Computationally, generating a matrix for a PV module with more than 48 cells generates a matrix that takes up more memory than what can be allocated on a standard computer, as the number of rows is in the order of $\approx 10^{14}$ or higher.

Repeat or duplicate scenarios are scenarios where the I-V characteristics of the shading scenarios match, and the power output (P_{mpp}) is thus the same. This assumes that all cells in the module are identical. The set of scenarios we get on eliminating duplicate scenarios is considered a set of unique

scenarios. To obtain these unique scenarios, we need to count the scenarios in an 'ascending' order, with the limit for each column/bypass string being the number of solar cells in that column/bypass string. This is demonstrated using an example of a solar cell having three bypass diodes and three solar cells in each bypass string; see Table 3.1. The total number of cells in the module is $3 \times 3 = 9$.

	String 1	String 2	String 3
No shaded cells	0	0	0
Affecting 1 string	0	0	1
	0	0	2
	0	0	3
Upto 2 strings	0	1	1
	0	1	2
	0	1	3
	0	2	2
	0	2	3
	0	3	3
Upto 3 strings	1	1	1
	1	1	2
	1	1	3
	1	2	2
	1	2	3
	1	3	3
	2	2	2
	2	2	3
	3	3	3

Table 3.1: Unique Scenarios for 3x3 PV module

We get 19 unique scenarios as per table 3.1. Here, scenario [0 0 1] is used as it is equivalent to [0 1 0] and [1 0 0]. In all three scenarios, only one cell is shaded in 1 bypass string, and the I-V characteristic is thus the same. These types of duplicate scenarios are termed 'equivalent' scenarios. Another example is seen in figure 3.1.

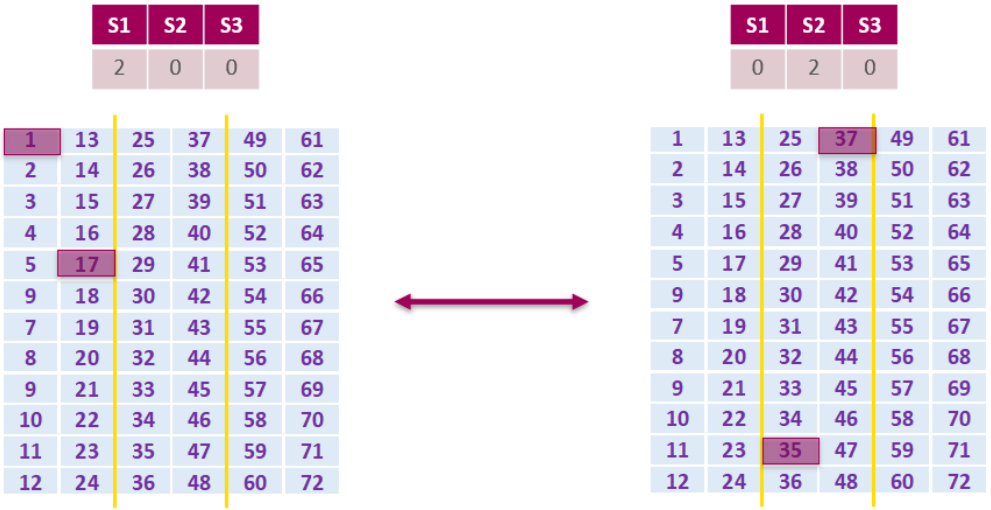

Figure 3.1: Example of equivalent scenario in a 72-cell module

To count the number of times equivalent scenarios occur, we have to consider all possible permutations of a scenario. The term permutation refers to a mathematical calculation of the number of ways a particular set can be arranged. In permutation, the order matters. For example, the number of ways 'a and b' can be arranged to occupy two positions without repetition is in two ways: ab and ba, as

the order in which they are presented matters. The number of permutations is defined by the formula, where r is the number of elements taken from a set of n elements:

$$ {}^{n}P_{r} = \frac{n!}{(n-r)!} \tag{3.1} $$

For equivalent scenarios, n and r are equal to the number of bypass diodes. In figure 3.1 we have a module with three bypass diodes that have some number of shaded cells in each string, and we wish to find how r=3 can be arranged in n=3 positions. Hence, for every unique scenario, r=n and number of permutations is ${}^{n}P_{n} = n!$. For 3 bypass diodes it is ${}^{3}P_{3} = 3!$ and for four bypass diodes it is ${}^{4}P_{4} = 4!$. Now, the unique scenario set might have scenarios with an equal number of shaded cells in different strings; for example, figure 3.1 [2 0 0] is one such scenario to occur in a three bypass diode PV module. When elements are repeated, the equation 3.1 is modified, and the number of permutations is:

$$ \frac{{}^{n}P_{n}}{\prod x_i!} = \frac{n!}{\prod x_i!} \tag{3.2} $$

where x_i is the number of times an element is repeated. If D is the number of bypass diodes, i is the number of elements, and n is the number of times the elements are repeated in the given unique shading scenario, the equation to calculate the number of equivalent scenarios of a unique scenario is thus defined as:

$$ \text{Equivalent scenarios} = \frac{D!}{\prod_{j=1}^{j=i} n_j!} \tag{3.3} $$

For the case of [2 0 0], D=3, i=2 (for 2 and 0) and, as 2 is repeated twice and 0 once, $n_1 = 2!$ and $n_2 = 1!$. The number of equivalent scenarios is

$$ \frac{{}^{3}P_{3}}{2! \times 1!} = \frac{3!}{2!} = 3 \tag{3.4} $$

Let us now consider equal scenarios. Equal scenarios are scenarios where the number of cells shaded in the bypass string will remain the same but can have different positions on the string. For example, the equal scenarios for the [2 0 0] are shown in figure 3.2.

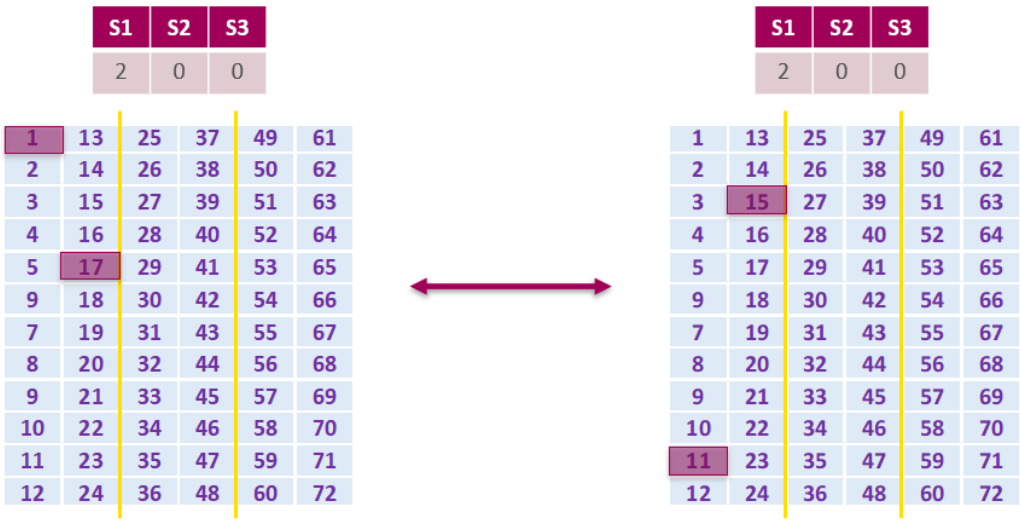

Figure 3.2: Example of equal scenarios in a 72-cell module

For r shaded cells in bypass strings of length N_s cells, we need to calculate the number of ways in which the assigned number of shaded cells per diode can form patterns. We are thus counting the number of all possible combinations given by the mathematical formula

$$ {}^{n}C_{r} = \frac{n!}{(n-r)! \times r!} \tag{3.5} $$

Using the equation 3.5, we get for one bypass diode:

$$\text{Number of combinations} = \frac{N_s!}{(N_s - r)! \times r!} \tag{3.6}$$

The number of possible equal scenarios of any given unique shading scenario for all **diodes** is the product of 3.6. The equation is defined as:

$$\text{Equal scenarios} = \prod_{d=1}^{d=D} \frac{N_s^d!}{(N_s^d - r_d)! \times r_d!} \tag{3.7}$$

For [2 0 0], D=3, $N_s = 24$ and $r_1 = 2$, $r_1 = 0$, and $r_1 = 0$ and the number of equal scenarios is:

$$\prod_{d=1}^{d=3} \frac{N_s^d!}{(N_s^d - r_d)! \times r_d!} = \frac{24!}{(24-2)! \times 2!} \times \frac{24!}{(24-0)! \times 0!} \times \frac{24!}{(24-0)! \times 0!} = 276 \tag{3.8}$$

From equations 3.3 and 3.7, the number of repeated scenarios (s_u) for a unique scenario is the product of the two, and the equation is:

$$s_u = \frac{D!}{\prod_{j=1}^{j=i} n_j!} \times \prod_{d=1}^{d=D} \frac{N_s^d!}{(N_s^d - r_d)! \times r_d!} \tag{3.9}$$

The number of repeat scenarios for [2 0 0] can now be calculated to be, from equations 3.4 and 3.8:

$$s_u = \frac{D!}{\prod_{j=1}^{j=i} n_j!} \times \prod_{d=1}^{d=D} \frac{N_s^d!}{(N_s^d - r_d)! \times r_d!} = 3 \times 276 = 828 \tag{3.10}$$

Using equation 3.10, we obtain the total number of repeated scenarios for every unique scenario to exist at the cell-level shading of a PV module. Thus, cell-level resolution is achieved, and we can proceed with calculating each cell's irradiance levels and temperatures for every shading scenario. The equation 1.2 to calculate ST can now be re-written as [1]

$$ST_{(i,c)} = \frac{1}{P_{mod,mpp}} \frac{1}{s_{u_{\text{total}}}} \sum_{u=1}^{u=u_{\text{total}}} P_{mpp_u} \cdot s_u \tag{3.11}$$

where

- u represents each unique scenario
- s_u is the number of times a unique scenario repeats
- P_{mpp_u} is the maximum power point of the PV module under that shading scenario
- $s_{u_{\text{total}}}$ is the total number of scenarios, which is simply equal to i^c
- $P_{mod,mpp}$ is the rated power of the module

3.1.3. Creating an irradiance and temperature matrix

Shading scenarios are not the only part of the code that needs to work at cell-level resolution. The PV module's irradiance level and temperature must also work at the cell-level resolution to obtain the I-V characteristics.

The code calculates the number of cells in each bypass string based on the number of bypass diodes and the total number of cells in the PV module. An initial layout of the exact cell resolution as the PV module is created, representing the unshaded irradiance layout for each bypass string. This layout is achieved by assigning an irradiance value of 1000 W/m^2 to the matrix based on the layout calculated earlier. In doing so, we created a standard irradiance map, with every row representing all cells in that string. We now use the unique scenario matrix found in section **??** to modify the shaded cells to have an irradiance value of 100 W/m^2. The number of cells to be modified per bypass string is taken from the value assigned in the respective column of that unique shading scenario.

Using the irradiance map made for all scenarios, obtaining a corresponding temperature map for cell-level resolution is possible. The function inputs irradiance matrices, the NOCT value, and ambient temperature to optimise the code. It calculates cell temperature matrices using the NOCT model and stores the results in the resulting cell temperature matrices. The code supports scenarios with varying ambient temperatures and single ambient temperature values.

3.2. Comparison of STs

Using the modifications described in section 3.1, we can calculate the value of ST for a PV module at cell-level resolution. Doing so affects the value of ST, and it is seen to decrease compared to c=12 significantly [1]. Figure 3.3 shows a comparison of five modules, each of different numbers of cells in series.

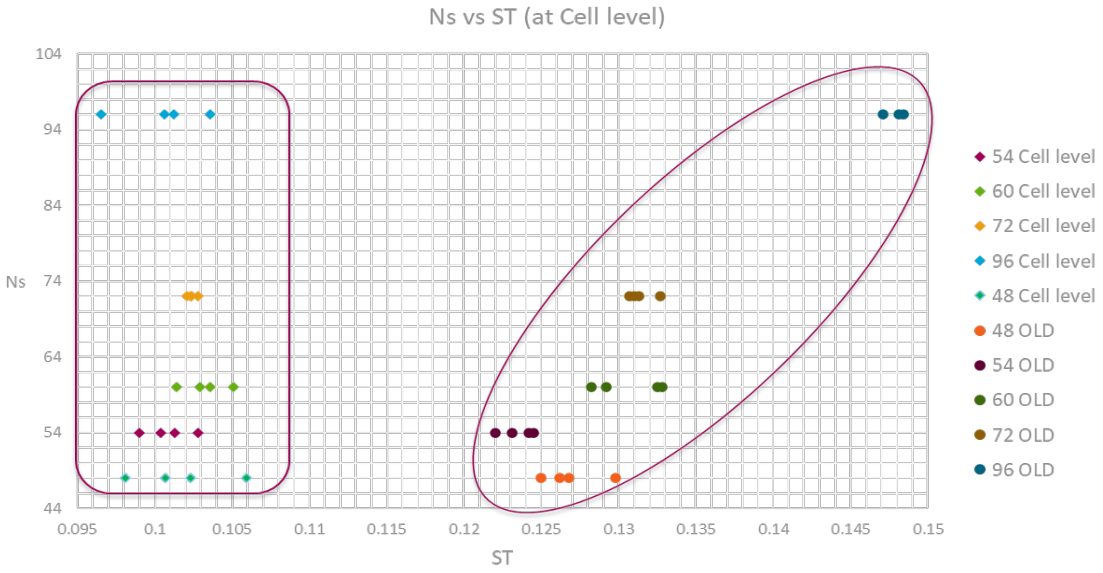

Figure 3.3: ST compared for c=12 and c=Ns

In the figure 3.3, we can see that ST values c = 12 show an increase in ST values with the increase in the number of cells in PV. However, ST values calculated at the cell level in the PV modules lie in the same range and show no relation between the number of cells in the module and the ST value calculated. To understand what may happen, closely examine the 48-cell PixonMP3 PV module. The module has 3 bypass diodes, with 16 cells in each string.

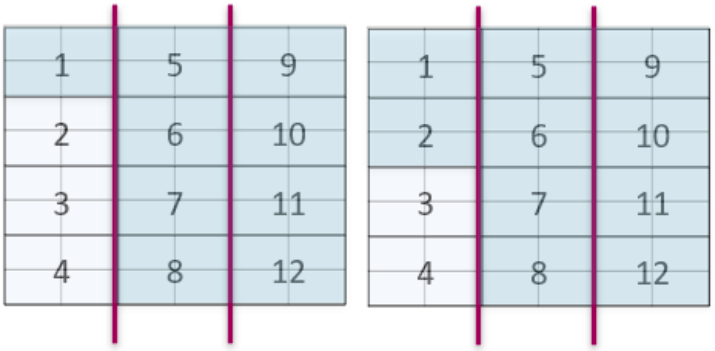

Figure 3.4: Shading scenario 25[1 4 4], 26[2 4 4] out of 35 possible scenarios for 48-cell PixonMP3 at c=12

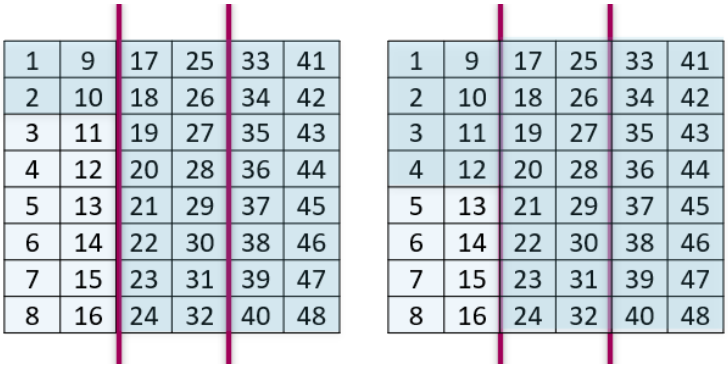

Figure 3.5: Shading scenario 605[4 16 16] and 805[8 16 16] out of 969 possible scenarios for 48-cell PixonMP3 at c=48

Figure 3.4 shows two unique shading scenarios that are consecutive in order at c=12 depth, while figure 3.5 shows their visual twin but at the cell level resolution. It should be noted that the scenarios at the cell level have 200 scenarios in between the two cases considered that are not otherwise counted when we have c=12 sections due to the difference in resolution.

ST is calculated using Equation 3.11 when we use the unique scenario set in the MATLAB model. Based on this equation, the number of unique scenarios u increases between the two shading scenarios shown in 3.5 is now 200 more when done for 3.4, and hence we get more terms of s_u. The value of $s_{u_{total}}$ is also increased. Overall, the ST value decreases because of the results seen in figure 3.3.

4

Validation

Validation is carried out to detect errors, protect data integrity and to ensure quality. Validation measurements for this ST model were carried out using the EternalSun large area solar simulator (LASS). Three modules were employed; the Trinasolar Duomax 144 half-cell module, the BenQ Sunforte 96-cell module and the JA Solar JAM6(K)(BK) 60-cell module. In section 4.1, the focus is on the half-cell module and in section 4.2, the focus is on the validation of the series connected PV modules. Validation is done by obtaining the I-V curve measured in the lab and comparing it against the I-V curve obtained by the MATLAB-based ST calculator.

4.1. Trinasolar Duomax 144 half-cell

The first module is the Trinasolar Duomax 144 half-cell, which has a butterfly layout. Experimental measurements were carried out using the LASS, while the model calculations were obtained using the ST calculator for 12 sections.

4.1.1. Half-cell technology

Half-cell technology is a subset of crystalline silicon technology [22]. They are a modification of the conventional crystalline silicon solar cell [23]. In half-cell, as the name suggests, the solar cell is cut in two equal halves through laser cutting. As the current generated by a cell is directly dependent on the area of the cell, half-cells produce a current that is equivalent to half the current generated by a complete cell[22, 23].

Losses due to the series resistance of cell connectors are directly influenced by the square of the current flowing through them. Consequently, by reducing the current by half, these losses decrease to one-fourth of their original magnitude [24, 25]. In addition to resistive losses, electrical losses also decrease due to the reduced cell distances and the more efficient use of space. In the cell-to-module concept, the reduced losses yield an increase of 0.48% in efficiency [23]. Thus series corrected half-cells produce slightly more power compared to half their number of complete cells [22, 25].

Half-cell PV modules typically have two sub-strings connected in parallel to one bypass diode. The modified configuration of bypass diodes impacts the possible shading scenarios that can be created.

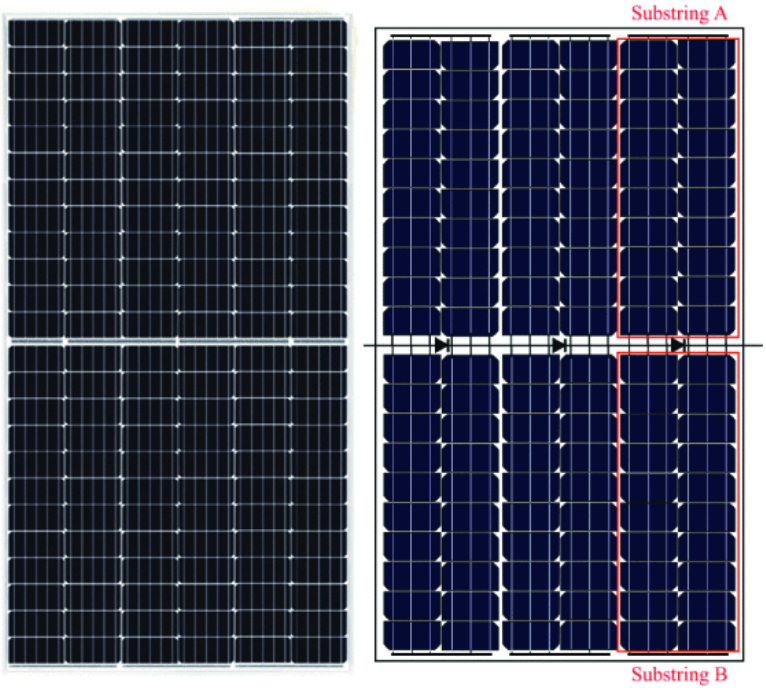

Figure 4.1: Half-cell PV module with six substrings and three bypass diodes

Figure 4.1 shows a schematic layout of the butterfly half-cell. In the diagram, there are two sets of 20 half-cells connected in series as substrings. These substrings are then connected in parallel to a bypass diode. The module contains a total of six substrings. This layout allows for two advantageous features:

- The output current of each string of the 120 half-cell module is comparable to the current output of each string of a conventional 60-cell module
- The presence of 6 substrings allows for an improved shading response

The shading response is improved since if shading occurs on half-cells in series in the same substring, they impact just one-sixth of the module's output. For a 60-cell standard module, an equivalent area shaded on the same string will however impact one-third of the module's output.

4.1.2. LASS Validation Trinasolar Duomax 144 half-cell

There are three cases shown here, one with no cells shaded, one with one-sixth of the module shaded and one with one-third of the module shaded. PV characteristic data from the datasheet is given in table 4.1 and verified in figure 4.4.

Pmax [W]	390
Vmpp [V]	40.2
Impp [A]	9.71
Voc [V]	48.5
Isc [A]	10.25

Table 4.1: Trina Solar DUOMAX 144 half-cell data

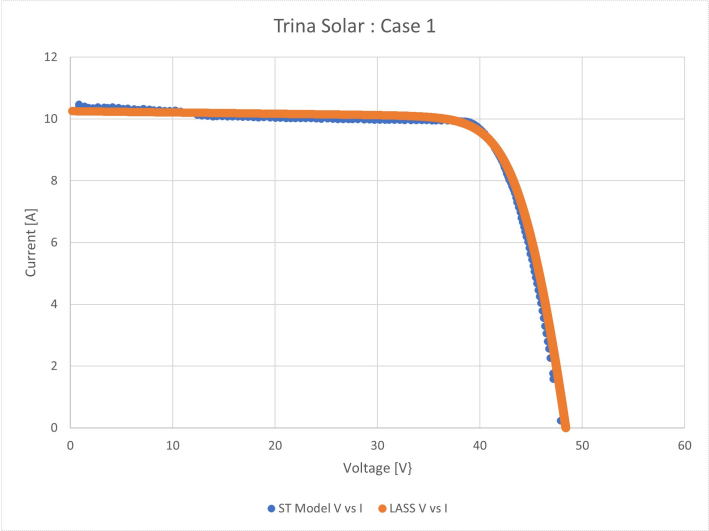

Figure 4.2: Case 1 of Trina Solar, I-V curve. Unshaded PV module

Figure 4.3: Case 1 of Trina Solar

Readings are taken for all three cases with the I-V curves showing minimal differences and can be used to validate the butterfly model of the MATLAB code. It is noted that the PV module used here is newly manufactured and has almost no ageing. Table 4.2 shows P_mpp values for all three cases.

	Number of Cells shaded	Number of bypass diodes active	LASS Pmmp [W]	ST model, c=12 Pmpp [W]	Error % vs measured values
[HTML]FFFFFFCase 1	0	0	387.6846	387.6846164	1.46623E-14
Case 2	24	1	247.6881	248.083404	0.159342
Case 3	48	2	210.946	220.6756369	4.612366869

Table 4.2: Pmpp values, measured and from the ST model

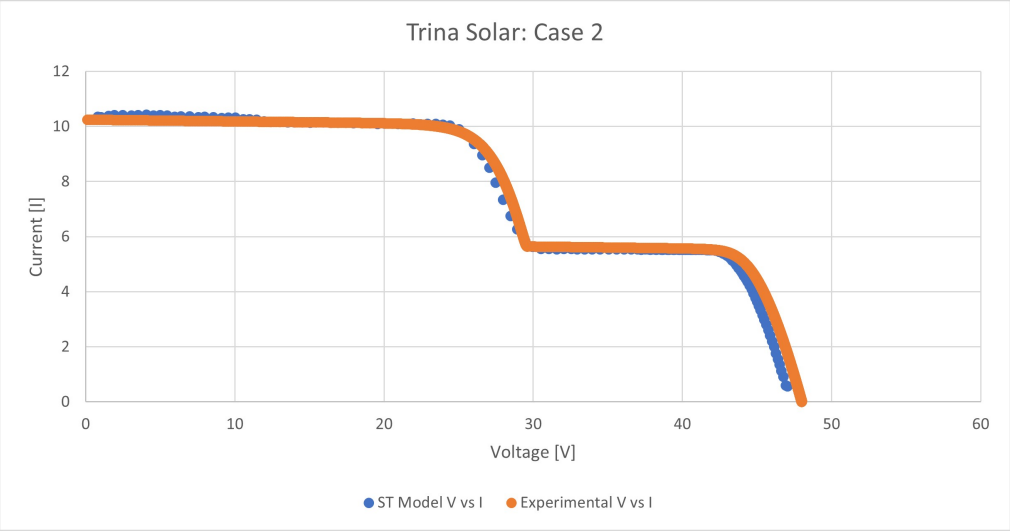

Figure 4.4: Case 2 of Trina Solar, I-V curve. One-sixth of PV module is shaded.

Figure 4.5: Case 2 of Trina Solar

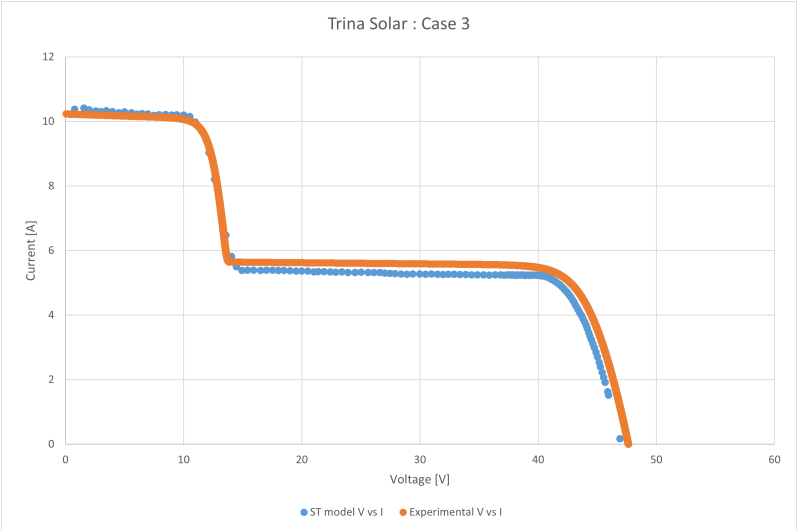

Figure 4.6: Case 1 of Trina Solar, I-V curve. One-third of PV module is shaded.

Figure 4.7: Case 3 of Trina Solar

All three cases show less than 5% error in P_mpp values and the I-V curves obtained have close values and similar curves.

4.2. JASolar JAM6 and BenQ Sunforte

For conventional PV modules, measurements were carried out to test shading scenarios of two types: clustered shading of rectangular shapes and shaded single and double-cell readings. The JASolar JAM is a 60-cell conventional PV module with three bypass diodes and having equal string length of 20 solar cells per bypass diode. The BenQ Sunforte is a 96-cell module with three bypass diodes but of unequal length. The BenQ module has solar cells arranged in 8 columns and 12 rows. The outer bypass diodes support two columns each while the bypass diode in the center supports 4 columns. The strings are of lengths 24 solar cells and 48 solar cells. It should be noted that unlike the Trina Solar 144 half-cell PV module, these two modules are much older and can possibly have ageing issues.

Shown in fig 4.8 is the first case, an unshaded JAM6 PV module. The curves obtained here have a visible difference in values and do not lie close to each other.

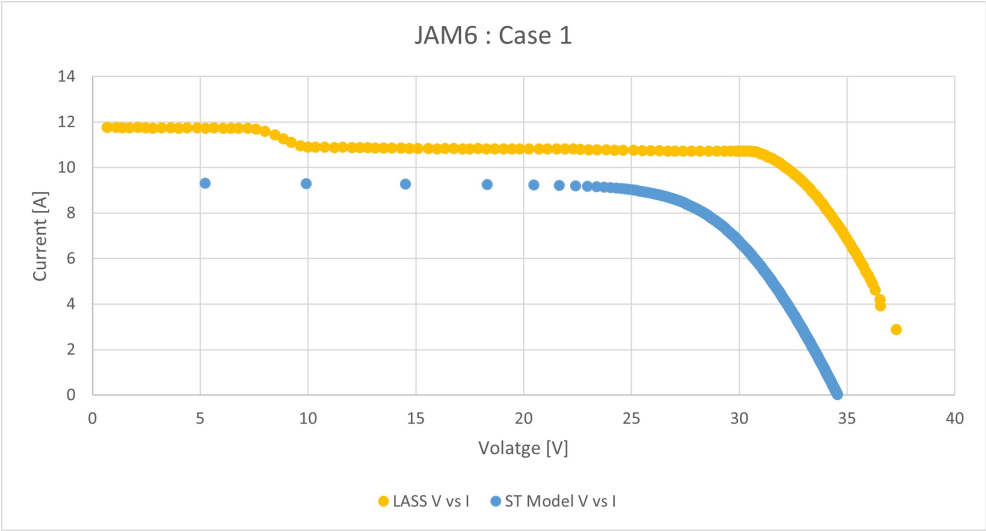

Figure 4.8: Case 1 of JASolar JAM6, I-V curve. Unshaded PV module

To see if the differences persisted in shaded scenarios, the I-V curve for one shaded cell (case 2) and two shaded cells (case 3) were plotted. In Both cases, the solar cells lie on the same string and thus activate just one bypass diode. In figures 4.9 and 4.10, the differences persist.

Both cases 2 and 3 have more steps in their plots than the expected I-V curve and indicate damaged

cells, or heavy mismatch, or defects in the bypass diodes. There is also a slight slope at I_{sc}, indicating that there may exist shunt paths that decrease shunt resistance [26].

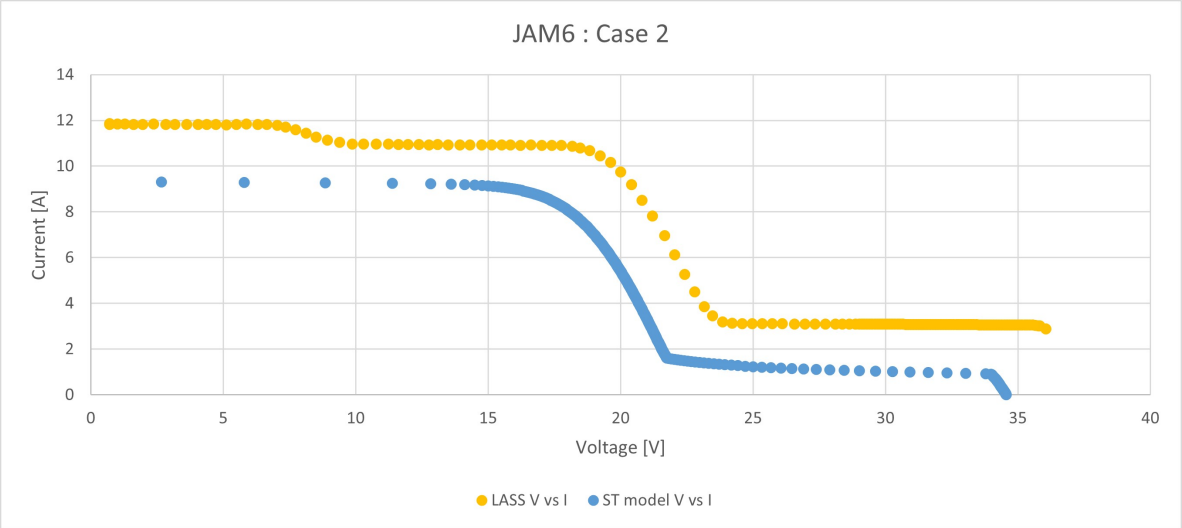

Figure 4.9: Case 2 of JASolar JAM6, I-V curve. One solar cell is shaded

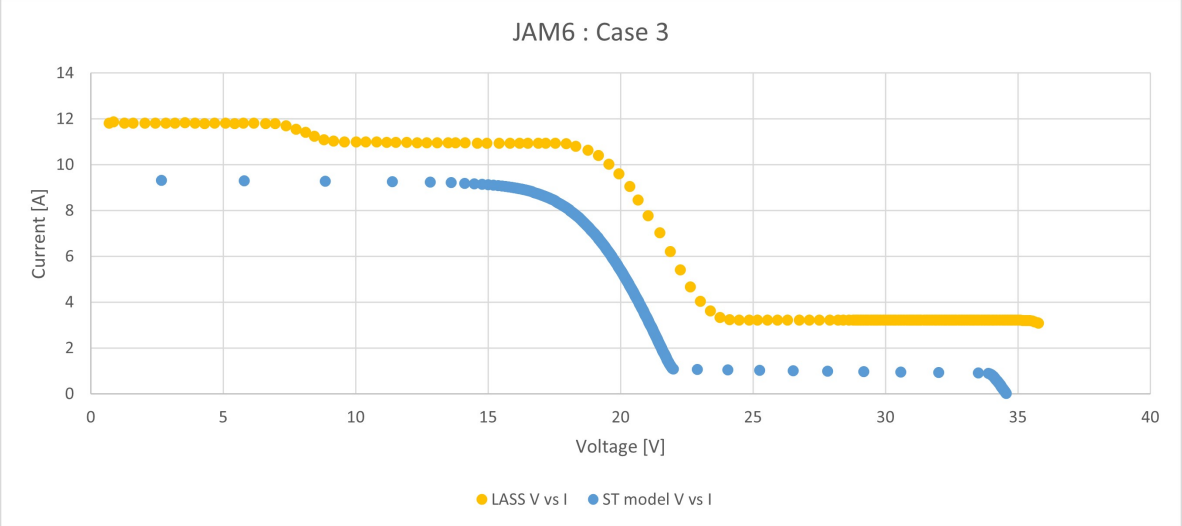

Figure 4.10: Case 3 of JASolar JAM6, I-V curve. Two solar cells are shaded

(a) Case 2 **(b)** Case 3

Figure 4.11: Experimental set-up for cases 2 and 3

Similar issues were seen in the 96-cell BenQ Solar PM096BOO module for the same scenarios. For cases where a larger fraction of the area was covered, the I-V curves obtained showed a rough curve. One of the scenarios considered was rectangular shadows to mimic shadows caused by obstacles in surroundings such as chimneys, other PV modules and taller buildings. In case 4 of BenQ solar, one-third of the PV module was covered with the shadow laid to fall across all three bypass diodes as shown in 4.13

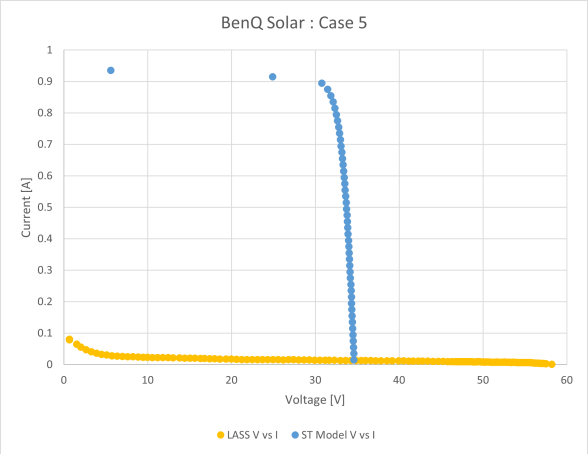

Figure 4.12: Case 5 of BenQ Solar, I-V curve. One-third of the module and shaded region lies across all three bypass diodes.

The LASS I-V curve reading for case 4 as seen in 4.12 is almost zero. The values taken from the LASS also show multiple peaks and steps when analysed. This indicates that the module may have some voltage noise, which due to the steep nature of the I-V curve causes the above-mentioned imperfections to be magnified in the current readings [27].

On comparing the results of the Trinasolar Duomax 144 half-cell module to that of the BenQ Sunforte 96-cell module and the JA Solar JAM6(K)(BK) 60-cell module, it is clear that module age does matter when carrying out validation measurements. The ST Model is a tool to calculate the shading tolerability of PV modules that manufacturers have produced and are available in the market. For the model to be validated successfully, the validation process requires the PV modules to be in the same condition as when the modules are being purchased. Due to the issues arising for two of the three modules, the validation process was only partially successful.

Figure 4.13: Case 4 of BenQ Solar

5

Sensitivity Analysis of ST

This chapter summarizes the sensitivity analysis tests done for selected 12 modules on the MATLAB-based code for three different variables in section **??**.

Table 5.1 shows the twelve modules that were selected to run the simulations. The ST values shown in table **??** are calculated for the base case. The base case variables have the same values as the ones given in their datasheet. The sensitivity analysis is carried out to study the impact of three input variables on the ST and the ST curve. The three variables are breakdown voltage (Vbr), nominal operating cell temperature (NOCT) and the number and configuration of bypass diodes.

Module	Ns	Cell-Tech	Config	BD	BD Config	Vbr	T_NOCT	ST
Aleo S_24	48	Poly c-Si	6x8	3	[2 2 2]	-18	47	0.102139
PAHAL49Series	48	Poly c-Si	6x8	3	[2 2 2]	-18	48	0.098962
Pixon PIX MP3 48	48	Mono c-Si (PERC)	6x8	3	[2 2 2]	-18	45	0.098105
TitanM6-54	54	Poly c-Si	6x9	3	[2 2 2]	-18	45	0.100236
JSkyE ST54-P230	54	Poly c-Si	6x9	3	[2 2 2]	-18	45	0.102684
Solarday PX54 250W	54	Poly c-Si	6x9	3	[2 2 2]	-18	43	0.101172
Tenesol TE 2200	60	Poly c-Si	6x10	3	[2 2 2]	-18	45	0.101307
Bisol Premium Series BMU	60	Poly c-Si	6x10	3	[2 2 2]	-18	44	0.104938
JASolar JAM6®(BK) 60/270	60	Mono c-Si	6x10	3	[2 2 2]	-18	45	0.102793
Qcells Q.PEAK-G5.1	60	Mono c-Si	6x10	3	[2 2 2]	-18	43	0.103276
TPL S-72 Series	72	Mono c-Si	6x12	3	[2 2 2]	-18	45	0.099329
DMEGC DM395G1-72SW	72	Mono c-Si (PERC)	6x12	3	[2 2 2]	-18	42	0.104202
Calrays CPM230-A-96	96	Mono c-Si	8x12	4	[2 2 2 2]	-18	45	0.103418
Topsola TSM96-125M	96	Mono c-Si	8x12	4	[2 2 2 2]	-18	45	0.101075
Panasonic module HIT (VBHN330SJ47)	96	HIT heterojunction cells	8x12	4	[2 2 2 2]	-18	44	0.10288
BenQ Sunforte PM096B00	96	Mono c-Si	8x12	3	[2 4 2]	-18	45	0.104202

Table 5.1: ST Results of select PV modules

To visualize the changes made in ST and to identify if there are any changes more significant in certain shading scenarios than others, the P_{mpp} values of each shading were plotted against the fraction of the area shaded.

5.1. Breakdown Voltage

Previously, we have discussed how bypass diodes activate when the overall voltage of the string drops below the forward voltage of the diode upon experiencing shading. When the reverse voltage of the string is high enough, the diode starts conducting current and voltage across the string is then limited to the forward voltage of the diode. This voltage at which the diode starts conducting current is called

Module	Ns	Cell-Tech	Config	BD	BD Config	Vbr	ST	Vbr	ST
Aleo S_24	48	Poly c-Si	6x8	3	[2 2 2]	-18	0.10213868	-3	0.10213871
PAHAL49Series	48	Poly c-Si	6x8	3	[2 2 2]	-18	0.09896217	-3	0.09896230
Pixon PIX MP3 48	48	Mono c-Si (PERC)	6x8	3	[2 2 2]	-18	0.09810504	-3	0.09811350
TitanM6-54	54	Poly c-Si	6x9	3	[2 2 2]	-18	0.10023628	-3	0.10023656
JSkyE ST54-P230	54	Poly c-Si	6x9	3	[2 2 2]	-18	0.10268352	-3	0.10268354
Solarday PX54 250W	54	Poly c-Si	6x9	3	[2 2 2]	-18	0.10117163	-3	0.10117356
Tenesol TE 2200	60	Poly c-Si	6x10	3	[2 2 2]	-18	0.10130653	-3	0.10130721
Bisol Premium Series BMU	60	Poly c-Si	6x10	3	[2 2 2]	-18	0.1049378	-3	0.10493882
JASolar JAM6® (BK) 60/270	60	Mono c-Si	6x10	3	[2 2 2]	-18	0.10279343	-3	0.10279438
Qcells Q.PEAK-G5.1	60	Mono c-Si	6x10	3	[2 2 2]	-18	0.10327617	-3	0.10327810
TPL S-72 Series	72	Mono c-Si	6x12	3	[2 2 2]	-18	0.09932894	-3	0.09932916
DMEGC DM395G1-72SW	72	Mono c-Si (PERC)	6x12	3	[2 2 2]	-18	0.10420247	-3	0.10420274
Calrays CPM230-A-96	96	Mono c-Si	8x12	4	[2 2 2 2]	-18	0.10341792	-3	0.10341792
Topsola TSM96-125M	96	Mono c-Si	8x12	4	[2 2 2 2]	-18	0.10107495	-3	0.10107495
Panasonic module HIT (VBHN330SJ47)	96	HIT heterojunction cells	8x12	4	[2 2 2 2]	-18	0.10287986	-3	0.10287997
BenQ Sunforte PM096B00	96	Mono c-Si	8x12	3	[2 4 2]	-18	0.10420247	-3	0.10420274

Table 5.2: Results for Vbr=-18V and Vbr=-3V

the breakdown voltage (Vbr) [28]. The lower the breakdown voltage, the more sensitive the diode is to the drop in voltage when shading occurs, and the diode can provide an alternate path for the current and mitigate the effects of partial shading.

Breakdown voltage (Vbr) in the base case is taken as -18V in the simulations for all 12 PV modules. This value is selected as, for most crystalline silicon solar cell technology, the breakdown voltage ranges from -13V to -20V, with a wider range of -10V to -30V also seen[29]. The value of Vbr = -18V can also be taken as the average value of front/back contacted crystalline silicon solar cells as the values of Vbr range from -13V to -18V [29, 30].

The ST values for both cases are shown in 5.2. There is negligible impact on the ST values and no direct relation is seen between Vbr and ST. A probable cause could be the number of solar cells in each bypass string. The effect of shading one solar cell is a decrease in the voltage by 0.5-0.8V [31]. However, if more cells are shaded, the voltage drop will increase and the advantage of a bypass diode will stagnate. As seen in figures 5.1 and 5.2, we get three plateaus that correspond to the number of bypass diodes that are active. The slope of the plateaus is insignificant and indicates that once a bypass diode is conducting current there are not many fluctuations occurring if more solar cells in the sting are shaded.

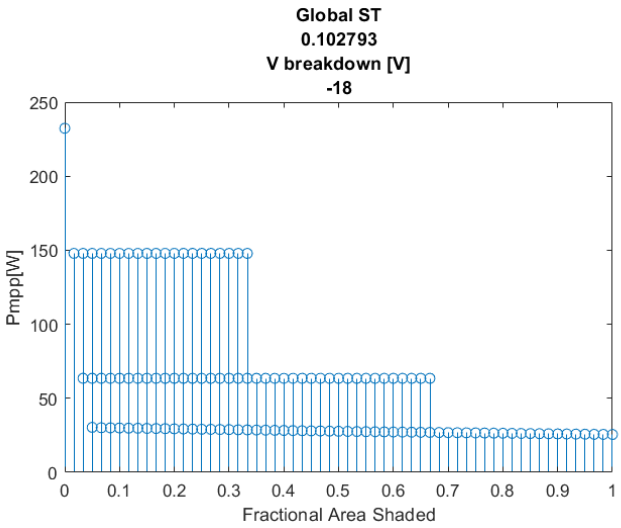

Figure 5.1: ST for Vbr=-18V for JASolar JAM6

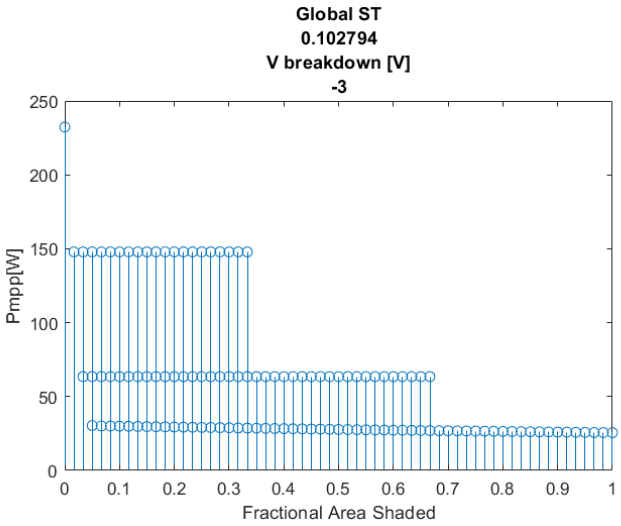

Figure 5.2: ST for Vbr=-3V for JASolar JAM6

Ideally, a PV module can achieve peak performance when the ratio number of the bypass diode to the number of solar cells is 1:1, which is economically infeasible [32]. It is further noted that a string of 4 solar cells is the most optimal outcome, and implementing this will increase the number of bypass diodes in a PV module [32].

5.2. Nominal Operating Cell Temperature (NOCT)

Nominal Operating Cell Temperature, abbreviated as NOCT, is a term given by the manufacturer in the datasheet as an estimate of the average cell temperature of a PV module. This temperature value corresponds to the temperature of a solar cell under an irradiance level of 800 W/m^2, an ambient temperature of 20 $^\circ$ C and an external wind speed of 1 m/s and is an alternative to the Standard Test Conditions[19]. The NOCT of a module can change due to changes in the ambient temperature and the manufactured physical characteristics [26].

The simulations were run for 5 different NOCT values, with the NOCT value being decreased in a step of 0.5 $^\circ$ C, with the first iteration being the given NOCT value in the datasheet. As the tempera-

ture was lowered, the value of ST was seen to linearly increase with the coefficient of determination (R^2) coming to approximately 1. It is to be noted that the ST calculator uses the temperature-sensitive two-diode module to generate the I-V curve which could be the reason for the strong value of R^2. In figures 5.3 and 5.4, we see the linear increase in ST as the NOCT value decreases.

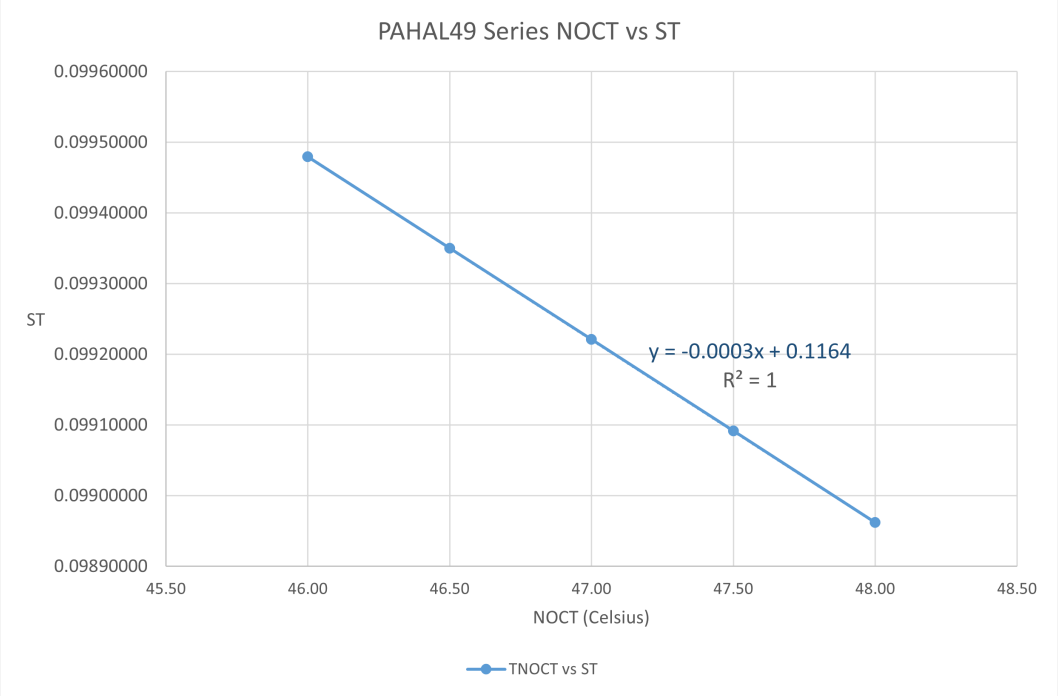

Figure 5.3: NOCT result for PAHAL49 Series, 48 cell PV module with given NOCT=48° C

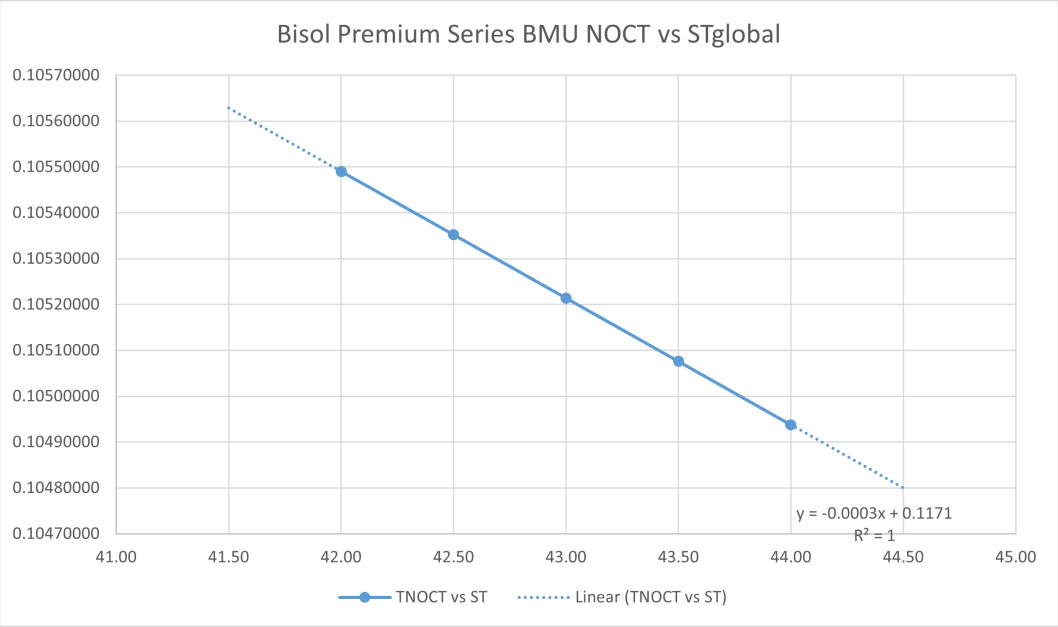

Figure 5.4: NOCT result for Bisol Premium BMU Series, 60 cell PV module with given NOCT=44° C

The values given by the NOCT simulations indicate a dependency of ST on cell temperature. However, the ST values by itself do not show any significant increase as NOCT decreases. The change in ST, though linear, is however negligible in impact.

5.3. Number of Bypass Diodes

Keeping in mind the possible limitations of computational threshold, the sensitivity analysis for bypass diodes is done by doubling the number of bypass diodes of the PV modules with equal bypass strings. The number of bypass diodes becomes either 6 or 8 diodes, depending on the value listed in table 5.1. As increasing the number of bypass diodes will also increase the unique scenario count, limiting the number of diodes to double the previous number allows for a comfortable simulation time to be run.

Module	Ns	Cell-Tech	Config	Vbr	BD	BD Config	ST	New BD	New BD Config	ST(New BD)
Aleo S_24	48	Poly c-Si	6x8	-18	3	[2 2 2]	0.10213868	6	[1 1 1 1 1 1]	0.10214351
PAHAL49Series	48	Poly c-Si	6x8	-18	3	[2 2 2]	0.09896217	6	[1 1 1 1 1 1]	0.09897077
Pixon PIX MP3 48	48	Mono c-Si (PERC)	6x8	-18	3	[2 2 2]	0.09810504	6	[1 1 1 1 1 1]	0.09806596
TitanM6-54	54	Poly c-Si	6x9	-18	3	[2 2 2]	0.10023628	6	[1 1 1 1 1 1]	0.10023883
JSkyE ST54-P230	54	Poly c-Si	6x9	-18	3	[2 2 2]	0.10268352	6	[1 1 1 1 1 1]	0.09950097
Solarday PX54 250W	54	Poly c-Si	6x9	-18	3	[2 2 2]	0.10117163	6	[1 1 1 1 1 1]	0.10117448
Tenesol TE 2200	60	Poly c-Si	6x10	-18	3	[2 2 2]	0.10130653	6	[1 1 1 1 1 1]	0.10130724
Bisol Premium Series BMU	60	Poly c-Si	6x10	-18	3	[2 2 2]	0.1049378	6	[1 1 1 1 1 1]	0.10493857
JASolar JAM6®(BK) 60/270	60	Mono c-Si	6x10	-18	3	[2 2 2]	0.10279343	6	[1 1 1 1 1 1]	0.10279418
Qcells Q.PEAK-G5.1	60	Mono c-Si	6x10	-18	3	[2 2 2]	0.10327617	6	[1 1 1 1 1 1]	0.10327711
TPL S-72 Series	72	Mono c-Si	6x12	-18	3	[2 2 2]	0.09932894	6	[1 1 1 1 1 1]	0.09932900
DMEGC DM395G1-72SW	72	Mono c-Si (PERC)	6x12	-18	3	[2 2 2]	0.10420247	6	[1 1 1 1 1 1]	0.10420254
Calrays CPM230-A-96	96	Mono c-Si	8x12	-18	4	[2 2 2 2]	0.10341792	8	[1 1 1 1 1 1 1 1]	0.10341792
Topsola TSM96-125M	96	Mono c-Si	8x12	-18	4	[2 2 2 2]	0.10107495	8	[1 1 1 1 1 1 1 1]	0.10107497
Panasonic module HIT (VBHN330SJ47)	96	HIT heterojunction cells	8x12	-18	4	[2 2 2 2]	0.10287986	8	[1 1 1 1 1 1 1 1]	0.10323431
BenQ Sunforte PM096B00	96	Mono c-Si	8x12	-18	3	[2 4 2]	0.10420247	6	NA	NA

Table 5.3: Results for sensitivity analysis done on number of bypass diodes

The increase in ST is again negligible, however on plotting the Pmpp values for every scenario on the y-axis against the fractional areas shaded of every scenario in the x-axis, the following graphs are shown below in figure 5.5. Increasing the number of bypass diodes increases the number of plateaus that form. These plateaus indicate how many number of bypass diodes get activated. On the left side of the graph, we can see that for a smaller fraction of the area shaded, the output power is higher for more scenarios.

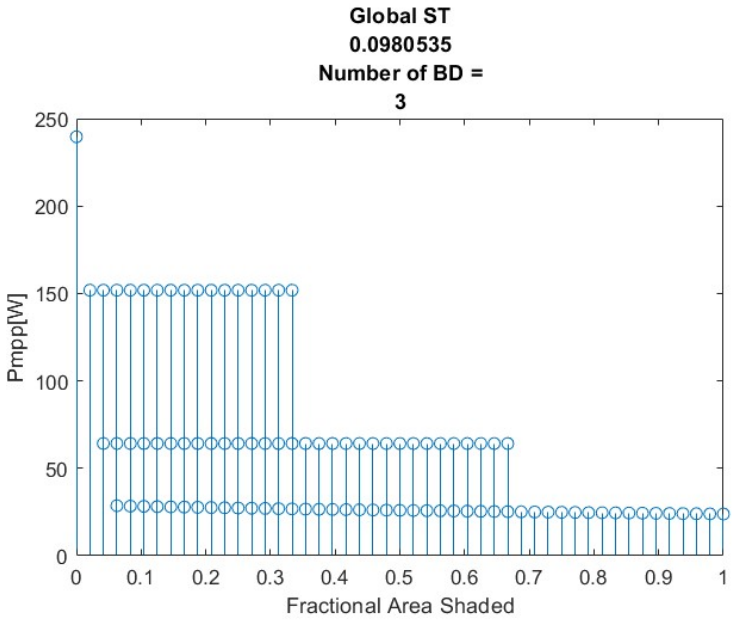

(a) (a))

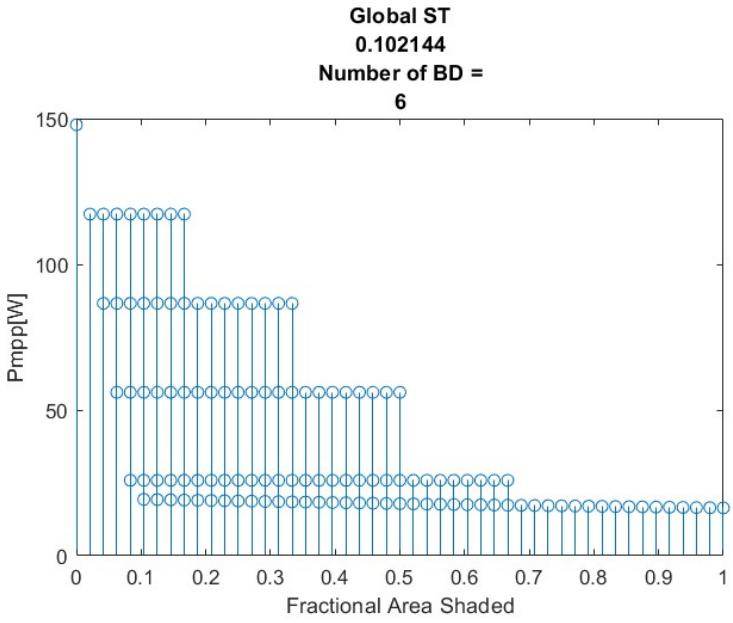

(b) (b)

Figure 5.5: Plot for, a)BD=3 and b)BD=6 for Pixon MP3 48 cell module

To better understand the impact of bypass diodes on the ST of the PV module, a local ST value is calculated only considering those shading scenarios where the fraction of shaded area scenarios does not exceed one-third of the total area of the module. The figure for this Local ST is shown in figure 5.6.

There is a visible increase in the value of the Local ST. The approximate percentage increase of ST local for the Pixon MP3 module is 6%. This shows that increasing the number of bypass diodes can help improve ST in certain scenarios.

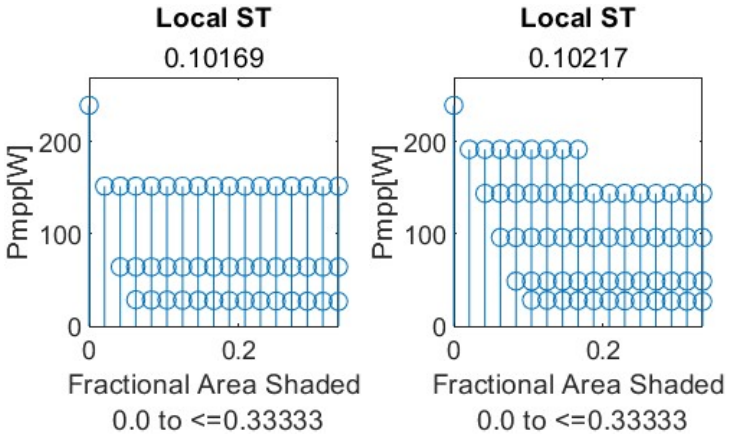

Figure 5.6: Plot for local ST, a)BD=3 and b)BD=6 for Pixon MP3 48 cell module

5.4. Guidelines for Improving ST

From the sensitivity analysis, the breakdown voltage and the NOCT have a negligible impact on ST when it is the sole factor being changed. but increasing the number of bypass diodes shows an increase in the local shading tolerance of PV modules. Apart from better performance, increasing the number of bypass diodes also allows the module to have a lower value of breakdown voltage due to having a lesser number of solar cells per string.

However, increasing them also has its own set of issues, mainly the increase in manufacturing cost and the increases in the number of local maximum peaks in the P-V curve. Tracking the global maxima also requires a complicated Maximum Power Point Tracking (MPPT) algorithm, which can be detrimental when one needs the MPP value in real-time [33]. Another issue is that bypass diodes also have their own conduction losses and increasing the number of bypass diodes will increase these losses, which can impact the efficiency of the PV module [34].

Work done by Aobaid et al. studied this optimization problem and developed a total utility value function to calculate the optimum number of bypass diodes. Total utility measures the satisfaction or benefits a person gets from the total consumption—including marginal utility—of a product or service. Based on the results of the normalized total utility value function for increasing the number of bypass diodes, the optimum configuration achieved for a 96-cell series connected PV module was 24 bypass diodes [32], showing that it is possible to improve the number of bypass diodes to a great extent.

It is thus recommended to have a higher number of bypass diodes to improve the performance of PV modules under partial shading.

6

Conclusions and Recommendations

This report mainly aimed to optimize the MATLAB-based ST calculator so that the ST calculator could be used to calculate ST at higher accuracy and to study the impact of PV module parameters on the value of ST. The objectives mentioned in the introduction are revised below and then further discussed if they were achieved. Lastly, further recommendations are mentioned for future research.

6.1. Conclusions

The following section outlines the primary objectives outlined in the chapter 1 and how they were achieved.

- **Optimization of the MATLAB-based ST calculator**: Improving the model's computational time was required to adapt the MATLAB model for calculating ST for a higher number of sections, which is necessary for greater accuracy. The study identified that using 'for' loops for data processing contributed the most to the computational time due to the presence of large matrices that stored required datasets. However, by implementing MATLAB's vectorization technique, which performs operations on entire arrays and takes advantage of optimized internal processes, code execution became significantly faster. This speed optimization reduced computational time to a few seconds when calculating ST for 12 sections, aligning to improve speed efficiency.

- **Adapting the ST calculator to work at cell-level irradiance and the impact of it on the ST parameter**: The main objective of this thesis was to adapt the MATLAB model to calculate ST for cell-level shading resolution. It was identified that the previous approach of identifying the unique scenarios from the set of all possible scenarios has a memory threshold for the number of sections $c = 48$ and cannot be applied at cell-level resolution for modules with a higher number of cells.
  It was decided first to generate a set of unique scenarios directly, and this method is explained in the sub-section 3.1.2. The number of times each unique scenario repeats itself in the set of all possible scenarios was then calculated using the mathematical concept of permutations. Two types of duplicate scenarios were observed in the context of modelling solar module performance under various shading conditions, equivalent scenarios and equal scenarios.
  Permutations were used to count equivalent scenarios, taking into account the order in which shaded cells appear. An equation is introduced to find the total number of equivalent scenarios for a unique scenario, considering the number of times each element (shaded cells in bypass strings) is repeated. The formula for counting equivalent scenarios is given in 3.3 and addresses the issue of duplicate counting. Equal scenarios, where the number of shaded cells in a bypass string remains the same, but the arrangement differs, are also discussed with the equation to calculate them defined as equation 3.7. The number of repeated scenarios for a unique scenario is calculated as a product of equivalent and equal scenarios, resulting in cell-level resolution for shading scenarios. This information is then used to calculate shading tolerability (ST) with a modified formula that accounts for the repetition of unique scenarios.

In conclusion, these mathematical formulations and calculations allow for a detailed analysis of solar module shading scenarios, enabling the determination of irradiance levels and temperatures for each cell under various shading conditions. This enhances the understanding of solar module performance and shading effects.

- **To study the relation of certain PV module parameters on the ST parameter by isolating their impact**: One key benefit of this model is that it allows for the separate examination of individual parameters in a PV module to understand how each parameter affects the shading tolerability (ST) value. A sensitivity analysis test was conducted to assess the influence of three input variables on ST and the ST curve. The input variables for the analysis are breakdown voltage, nominal operating cell temperature (NOCT) and the number of bypass diodes.
  A base case of ST values was generated using datasheet inputs for 16 PV modules given in table 5.1. To visualize the changes in ST and identify significant variations in different shading scenarios, Pmpp values (maximum power point) are plotted against the fraction of shaded area for each scenario.
  The results in Table 5.2 indicate that breakdown voltage has negligible impact on ST, with no clear correlation observed. This lack of correlation may be attributed to the number of solar cells in each bypass string, as shading a single cell results in a modest voltage drop. Still, the advantage of a bypass diode diminishes as more cells are shaded. The graphs in Figures 5.1 and 5.2 illustrate plateaus in the ST curve corresponding to the number of active bypass diodes, indicating that further fluctuations are minimal once a bypass diode is conducted.
  Sensitivity analysis done for NOCT was conducted for five different NOCT values, with a 0.5 stepwise decrease from the datasheet NOCT value. It revealed a linear increase in shading tolerability (ST) as NOCT decreases, although the impact of this change on ST was negligible.
  Sensitivity analysis of bypass diodes identified that increasing the number of bypass diodes in PV modules can enhance shading tolerance. A sensitivity analysis was performed by doubling the number of bypass diodes for the PV modules listed in table 5.1, resulting in 6 or 8 bypass diodes. The outcomes of this sensitivity analysis showed a slight increase in shading tolerance (ST) as the number of bypass diodes increased. Plotting Pmpp values against the fractional shaded area for various scenarios revealed the formation of plateaus corresponding to the activation of bypass diodes. These plateaus indicated that more scenarios achieved higher output power for a smaller fraction of the area shaded. To further explore the influence of bypass diodes on PV module ST, a local ST value was calculated for scenarios where the shaded area did not exceed one-third of the module's total area. The results showed a noticeable increase in the Local ST. This suggests that increasing the number of bypass diodes can be beneficial in specific shading scenarios.

- **Find guidelines to improve the shade tolerance of PV modules**: One of the objectives of this thesis was to suggest approaches to enhance ST. Based on the results found in chapter 5, it was recommended to increase the number of bypass diodes to improve the shading tolerability of PV modules, but this improvement has drawbacks such as increased manufacturing costs, complexity in maximum power point tracking (MPPT) algorithms, and conduction losses, as highlighted in section 5.1.1..

6.2. Further Recommendations

Below are some recommendations for potential future areas of research and for improving this work.

- **Validation measures**: It has been noted that the LASS has produced insufficient results for two out of three modules, likely due to their age. This highlights the need for new modules to be used for validation purposes. Additionally, it is important to mention that the MATLAB model calculates ST based on newly manufactured modules. Conducting validation on these new modules enables a more accurate comparison of experimental results with those generated by the MATLAB model.

- **Irradiance Levels**: Currently, the shading tolerance (ST) calculation involves the consideration of two irradiance levels. Ziar et al. demonstrated, through both mathematical analysis and experimentation, that the observed trends with these two irradiance levels should hold true as the

irradiance levels approach infinity. Nevertheless, it could be intriguing to investigate the effects of using 3, 4, or more irradiance levels in the ST calculation to determine if they influence the ST of various modules.

- **Adapting ST model for additional PV module layouts** The main objective of this report was to adapt the model for calculating ST at cell-level resolution for series connected ST. PV modules with a butterfly connection layout or shingled cell layouts exist on the market and have shown a higher tolerance for shading compared to conventional series-connected modules. Adapting the model to work for more layouts will allow for the objective comparison of different modules and expand the database of ST values that can be generated.

- **Improving section resolution and shading scenarios**: The current ST calculator can calculate ST for cell-level resolution, however improving this further to sub-cell resolution will allow for a smoother ST curve to be generated when plotting the P_{mpp} for every shading scenario against the fractional area shaded. A sub-cell resolution will potentially achieve an ST plot that shows a curve rather than the plateaus that are seen in current graphs.

- **Analysis for the impact of Breakdown Voltage and Bypass Diode together on ST**: In this report, we analyzed how Vbr and the number of bypass diodes impact the efficiency of solar cells. It was found that there is a dependency between the two factors, as increasing the number of bypass diodes may lower the breakdown voltage and reduce the number of cells covered per diode. By analyzing ST with different values for both factors, we can take advantage of this benefit and improve the overall ST value.

- **Development of mathematical expression for λ**: The current model allows for the assessment of how individual parameters affect shading tolerability (ST). This allows for the possibility of creating a mathematical expression for λ, which has not been extensively studied yet. By using this approach, we can analyze how each parameter independently affects the ST of a module and how they may interact or offset each other. This provides a thorough examination of the parameters that contribute to ST and their relationships with λ.

Some recommendations for future work areas are mentioned below.

- **Modeling of Temperature and Hotspots**: The current ST calculator uses the NOCT model to generate cell temperature and model temperature as it was easy to integrate into this model. However, it also entails certain simplifications. Using a more comprehensive temperature model for cell temperature calculation could potentially improve the accuracy of the shading tolerance (ST) estimation. Partial shading conditions can elevate the temperature in and around shaded cells due to power dissipation, leading to hotspots. Introducing a model that could incorporate temperature changes resulting from partial shading into the model could further improve the accuracy of module temperature and, consequently, the calculated ST.

- **Module aging and time impact**: The occurrence of hotspots and other mechanical wear a tear that a module experiences impacts the output power of a module over time. It could be interesting to incorporate the impact of module degradation over time into the model when calculating the value of ST. This could also allow the calculation of time-dependent ST for different environments such as high or low- ambient temperature, etc.

References

[1] Nida Rukshi. *Development of a calculation tool to determine the shading tolerability of PV modules*. 2022.

[2] *PVEducation - Solar Energy*. online. URL: https://www.pveducation.org/pvcdrom/introduction/solar-energy.

[3] European Union. *Solar Energy*. 2022. URL: https://energy.ec.europa.eu/topics/renewable-energy/solar-energy_en.

[4] IEA (2022). *Approximately 100 million households rely on rooftop solar PV by 2030*. 2022. URL: https://www.iea.org/reports/approximately-100-million-households-rely-on-rooftop-solar-pv-by-2030%22.

[5] Zuo Wang et al. "Quantitative estimation of mismatch losses in photovoltaic arrays under partial shading conditions". In: *Optik* 203 (2020), p. 163950.

[6] Khaled Osmani et al. "Mitigating the effects of partial shading on PV system's performance through PV array reconfiguration: A review". In: *Thermal Science and Engineering Progress* 31 (2022), p. 101280.

[7] Romênia G Vieira et al. "A comprehensive review on bypass diode application on photovoltaic modules". In: *Energies* 13.10 (2020), p. 2472.

[8] Fei Lu et al. "Improved PV module performance under partial shading conditions". In: *Energy Procedia* 33 (2013), pp. 248–255.

[9] Pieter Bauwens and Jan Doutreloigne. "NMOS-based integrated modular bypass for use in solar Systems (NIMBUS): Intelligent bypass for reducing partial shading power loss in solar panel applications". In: *Energies* 9.6 (2016), p. 450.

[10] Timothy J Silverman et al. "Damage in monolithic thin-film photovoltaic modules due to partial shade". In: *IEEE Journal of photovoltaics* 6.5 (2016), pp. 1333–1338.

[11] Sofia Antunes Alves dos Santos et al. "The impact of aging of solar cells on the performance of photovoltaic panels". In: *Energy Conversion and Management: X* 10 (2021), p. 100082.

[12] Hesan Ziar et al. "Quantification of Shading Tolerability for Photovoltaic Modules". In: *IEEE Journal of Photovoltaics* 7.5 (2017), pp. 1390–1399. DOI: 10.1109/JPHOTOV.2017.2711429.

[13] Miguel García et al. "Solar-tracking PV plants in Navarra: A 10 MW assessment". In: *Progress in photovoltaics: Research and Applications* 17.5 (2009), pp. 337–346.

[14] Kristijan Brecl, Matevž Bokalič, and Marko Topič. "Annual energy losses due to partial shading in PV modules with cut wafer-based Si solar cells". In: *Renewable Energy* 168 (2021), pp. 195–203.

[15] Alberto Leon-Garcia. *Probability and random processes for electrical engineering*. Third. Pearson Education India, 1994.

[16] Sandeep Mishra et al. "Selection map for PV module installation based on shading tolerability and temperature coefficient". In: *IEEE Journal of Photovoltaics* 9.3 (2019), pp. 872–880.

[17] Nils Klasen et al. "A comprehensive study of module layouts for silicon solar cells under partial shading". In: *IEEE Journal of Photovoltaics* 12.2 (2022), pp. 546–556.

[18] J. Suganya and M. Carolin Mabel. "Maximum power point tracker for a photovoltaic system". In: (2012).

[19] Arno Smets et al. *Solar Energy: The physics and engineering of photovoltaic conversion, technologies and systems*. Bloomsbury Publishing, 2016.

[20] *JAM6(R)(BK)*. datasheet.

[21] *Vectorization*. URL: https://www.mathworks.com/help/matlab/matlab_prog/vectorization.html.

[22] Daniel de B Mesquita et al. “A review and analysis of technologies applied in PV modules”. In: *2019 IEEE PES Innovative Smart Grid Technologies Conference-Latin America (ISGT Latin America)*. IEEE. 2019, pp. 1–6.

[23] Arati Joshi, Afrah Khan, and SP Afra. “Comparison of half cut solar cells with standard solar cells”. In: *2019 Advances in Science and Engineering Technology International Conferences (ASET)*. IEEE. 2019, pp. 1–3.

[24] S Guo et al. “A quantitative analysis of photovoltaic modules using halved cells”. In: *International Journal of Photoenergy* 2013 (2013).

[25] Hamed Hanifi, Jens Schneider, and Jörg Bagdahn. “Reduced shading effect on half-cell modules—Measurement and simulation”. In: *31st European Photovoltaic Solar Energy Conference and Exhibition*. EU PVSEC. 2015, pp. 2529–2533.

[26] Vat Sun et al. “A new method for evaluating nominal operating cell temperature (NOCT) of unglazed photovoltaic thermal module”. In: *Energy reports* 6 (2020), pp. 1029–1042.

[27] AR Burgers et al. “Improved treatment of the strongly varying slope in fitting solar cell IV curves”. In: *Conference Record of the Twenty Fifth IEEE Photovoltaic Specialists Conference-1996*. IEEE. 1996, pp. 569–572.

[28] Darren Ashby. *Electrical Engineering 101 (Third Edition)*. Newness, 2012, pp. 67–131.

[29] Andres Calcabrini et al. “Low-breakdown-voltage solar cells for shading-tolerant photovoltaic modules”. In: *Cell Reports Physical Science* 3.12 (2022).

[30] Andres Calcabrini et al. “The relevance of the cell’s breakdown voltage in the dc yield of partially shaded pv modules”. In: *2021 IEEE 48th Photovoltaic Specialists Conference (PVSC)*. IEEE. 2021, pp. 0092–0094.

[31] Sukumar Mishra and Dushyant Sharma. *Electric Renewable Energy Systems*. 2016, pp. 457–486.

[32] Aisha Alobaid and Raymond Adomaitis. “Monte Carlo simulation for optimal solar cell configuration”. In: *Computer Aided Chemical Engineering*. Vol. 44. Elsevier, 2018, pp. 1855–1860.

[33] S Zahra Mirbagheri Golroodbari, Arjen C De Waal, and Wilfried GJHM Van Sark. “Improvement of shade resilience in photovoltaic modules using buck converters in a smart module architecture”. In: *Energies* 11.1 (2018), p. 250.

[34] Raoul Weegink. *Next Generation Shade-Tolerant Reconfigurable PV Modules for Urban Landscapes*. 2019.